


 Cite this: *Sens. Diagn.*, 2025, 4, 555

## A review on breast cancer diagnostic techniques

 Parikshana Mathur, <sup>a</sup> Saakshi Dhaneekar <sup>\*abc</sup> and B. D. Malhotra <sup>de</sup>

Breast cancer occurs when cells grow abnormally and form tumors. It is currently one of the most prevalent cancers in women, and it is known to cause serious detrimental effects if not detected on time. Thus, early detection and screening may tremendously contribute to a patient's medical treatment. The boom in cancer diagnostics resulted from the demand to overcome the limitations of bulky and time-consuming conventional detection methods. The new and advanced methods are simpler, faster and easily deployable. This review elucidates various techniques used for breast cancer detection, which include optical, electrochemical, mechanical, electrical, thermal and color- and breath-based methods. An overview of different techniques is presented with additional information related to the available commercial options. This review also presents the integration of artificial intelligence and Internet of Things into futuristic diagnostic techniques. The unmet needs and challenges are also discussed. Overall, this review is a comprehensive package for researchers who want to dive into the advances of breast cancer diagnostics.

 Received 7th February 2025,  
 Accepted 1st May 2025

DOI: 10.1039/d5sd00016e

[rsc.li/sensors](https://rsc.li/sensors)

### 1. Introduction

Breast cancer (BrC) is a type of tumor that generally occurs in the inner lining of epithelial tissues, milk ducts, and/or lobules. The reason for its occurrence is linked to several factors, such as inheritance of mutations in the genes, past exposure to radiation, and hormonal imbalance. It has now become the foremost cause for cancer-linked illnesses and mortality in females.<sup>1</sup> According to the WHO reports of 2024, it was the most common cancer in women with 670 000 deaths reported worldwide in recent times.<sup>2</sup> Early screening and diagnosis may improve the treatment efficiency. However, majority of the tests carried out in hospital laboratories are time-consuming and expensive.<sup>3</sup> The tests recommended for the detection of BrC at an early stage require professionally trained personnel to operate on bulky equipment, such as those used for ultrasounds, MRI, and mammograms, which are presently not easily affordable by the mass population. Further, the presence of specific BrC biomarkers (e.g., HER2, ER, PR, CA15-3, and CD44) formidably demands precise detection.<sup>4</sup> Owing to these

limitations and an urgent need for improvement in the current diagnostics, the research focus has shifted towards the development of detection techniques that are relatively less painful, more accurate, affordable, rapid, and easy to use with a low limit of detection. In addition to this, with the advent of nanotechnology, the use of nanoparticles has become prominent in various BrC detecting methods owing to their small size and unique physiochemical properties.<sup>5</sup>


**Parikshana Mathur**

*Parikshana Mathur obtained her BSc from JNVU, Jodhpur, and MSc and PhD from IIS deemed to be University, Jaipur. She secured a gold medal for her Master's and has trained at DRDO, Jodhpur. She has served as an Assistant Professor at Central University of Rajasthan in the Department of Biotechnology. Later, she worked as a Research Scientist at Sensekri Technology Solutions Pvt. Ltd., Technology Innovation*

*and Start-up Centre (TISC), IIT Jodhpur. Currently she is working as a Postdoctoral Fellow at Durban University of Technology, South Africa. She has published several research papers in reputed journals and 9 book chapters. Her past work involves plant-microbe interaction, endophytes, metabolomics and nanoparticle synthesis. Her current and future research interests include target-specific drug delivery and biosensors for societal applications.*

<sup>a</sup> Sensekri Technology Solutions Pvt. Ltd., Technology Innovation and Start-up Centre (TISC), IIT Jodhpur, NH 62, Nagaur Road, Karwar, Jodhpur 342030, Rajasthan, India. E-mail: saakshi@iitj.ac.in

<sup>b</sup> Inter Disciplinary Research Division – Smart Healthcare, IIT Jodhpur-AIIMS Jodhpur, NH 62, Nagaur Road, Karwar, Jodhpur 342030, Rajasthan, India

<sup>c</sup> Department of Electrical Engineering, IIT Jodhpur, NH 62, Nagaur Road, Karwar, Jodhpur 342030, Rajasthan, India

<sup>d</sup> Environmental Sciences & Biomedical Metrology, CSIR-National Physical Laboratory, Dr K.S. Krishnan Road, New Delhi 110012, India

<sup>e</sup> Department of Biotechnology, Delhi Technological University, Main Bawana Road, Delhi 110042, India



This review will take readers through a wide variety of recent techniques that are currently used for BrC diagnostics and their advantages and disadvantages (Table 1). Different aspects of sensing, commercial kits and future perspectives with an essence of AI and IoT methods used for BrC detection are covered.

## 2. Techniques in breast cancer (BrC) screening and diagnosis

### 2.1 Color-based techniques

**2.1.1 Lateral flow immunoassay (LFIA).** LFIA is a paper-based, qualitative, labelled, cost-effective, point-of-care diagnostic technique.<sup>21</sup> It is an immunochromatographic assay that facilitates the separation, capture, and detection of the target analyte. The intensity of colored lines on the LFA strip is directly related to the specific amount of analytes received and reacted upon.<sup>22</sup> The design of LFIA structure uses a strip (nitrocellulose membrane), primary and secondary antibodies and labels for the detection of target analytes.

Conventionally, gold nanoparticles have been used as labels. However, considering their cost, other materials such as graphenes have also been explored.<sup>23</sup> The most significant advantage of this method is that it provides real-time information, can be read by the naked eye and is extremely rapid in delivering results.

The traditional LFIAs can be used for the naked observation of qualitative or semi-quantitative results for samples having concentration above that of the assay. For

quantitative analysis of the targets, the advancements in LFIA techniques have emerged, which are employed with portable optical readers. Ye *et al.* have developed a sandwich LFIA-based HER2 immunosensor, wherein HER2-ECD protein in serum was detected with a limit of detection (LOD) of 1.7 ng mL<sup>-1</sup>, and detection in the range of 1.7 to 400 ng mL<sup>-1</sup> using a portable sensing method.<sup>24</sup> Another such advancement is fluorescent LFIA presented by Deng *et al.* they have synthesized second near-infrared (NIR-II) Ag<sub>2</sub>Se polystyrene beads that can be used as a fluorescent probe in LFIA for fast (within 15 min) and accurate detection of BrC markers (CEA and CA153) with a very low limit of detection (CEA: 0.768 ng mL<sup>-1</sup>, CA153: 1.192 U mL<sup>-1</sup>) and high recoveries (93.7% ± 6.2% to 108.8% ± 4%). This method is suitable for clinical and quantitative detection.<sup>25</sup>

Wang and co-workers created an optofluidic metasurface composed of silicon nanoposts (SNP) for lateral flow-through identification of BrC biomarker *ErbB2*. It consists of a top thin silicon layer, with a coating of graphene oxide (GO) nanosheets functionalized with anti-*ErbB2* (Fig. 1a). The GO coating enhances the loading capacity of anti-*ErbB2* molecules due to the presence of oxygenated groups like -COOH and -CHO, which assist in covalent bond formation with anti-*ERbB2* through EDC-NHS coupling. The analyte-ligand binding is monitored from the shift in the wavelength as observed in the reflectance spectra. The shift was apparently displaced in case of bare SNP to SNP with anti-*ErbB2* (Fig. 1b). The resonance dip shifts to longer wavelengths with the increase in *ErbB2* concentration (Fig. 1c). The dose-response curve and reflectance spectra, as



Saakshi Dhanekar

Saakshi Dhanekar received her PhD degree in Electronics from the Faculty of Engineering, Jamia Millia Islamia, New Delhi, India, in 2012. She has been with the Centre for Applied Research in Electronics (CARE) and the Centre for Biomedical Engineering (CBME), Indian Institute of Technology, New Delhi, from 2013 to 2019. She has been an Associate Professor at the Department of Electrical Engineering, IIT Jodhpur, India,

since 2019. She has more than 40 publications, four granted patents, and a few patents at different stages of evaluation in the field of sensors and diagnostics. Her research interests include sensor development using nanostructured silicon, metal oxides, IoT, and MEMS for industry and healthcare applications. She is the co-Founder and the Director of Sensekriti Technologies Solutions Private Ltd. She is actively working on diagnostic systems for the detection of diseases through non-invasive breath tests.



B. D. Malhotra

Dr B. D. Malhotra received his PhD from the University of Delhi, Delhi in 1980. Dr Malhotra has published more than 250 refereed papers in international journals, has filed 10 patents, and has edited/co-edited books on biosensors, organic nanocomposites and polymer electronics. His research papers are cited widely and carry an h-index of 98. Prof. Malhotra has established the internationally recognized Department of Science

& Technology Centre on Biomolecular Electronics at the CSIR-National Physical Laboratory, New Delhi, India. He is a recipient of the National Research Development Corporation Award 2005 for the invention of 'blood glucose biochemical analyzer', is a Fellow of the Indian National Science Academy, National Academy of Sciences, India and Academician of Asia Pacific Academy of Materials. His current research activities include nanobiomaterials, biosensors, ordered molecular assemblies, conducting polymers, Langmuir-Blodgett films, self-assembled monolayers, nano-biotechnology, biomedical engineering and biomolecular electronics.



**Table 1** Advantages and limitations of various techniques used for breast cancer screening

| Technique                     | Advantage   | Limitation   | Ref. |
|-------------------------------|---|--|------|
| LFIA                          | Cost-effective, point of care   | Semi-quantitative with possibility of cross-reactivity   | 6    |
| Flow cytometry                | High sensitivity with multiparameter analysis                             | Complex sample preparation   | 7    |
| SERS                          | Highly sensitive and specific   | Reproducibility and standardization of the SERS signal   | 8    |
| ELISA                         | Can be observed with naked eye  | Less sensitive   | 9    |
| Fluorescence-based techniques | Chromosomal aberration at single cell level can be analysed               | Provide semi-quantitative results  | 9    |
| <sup>1</sup> H-MRS            | Detailed soft tissue imaging without ionizing radiation exposure          | Time consuming, expensive, lack of anatomical information  | 10   |
| EIT                           | Generates tomographic image using non-ionizing radiation                  | Poor spatial resolution  | 11   |
| Electrochemical techniques    | Real-time monitoring, and cost-effective                                  | Less sensitive   | 12   |
| Breath-based techniques       | Easy sample collection  | Time-consuming data processing, less specificity   | 13   |
| MEMS                          | Highly sensitive real time measurement with minimal sample consumption    | Lack of standardization, complex fabrication leading to increased cost                                     | 14   |
| PMUTs                         | Reduced size, enhanced bandwidth and sensitivity, lower power consumption | Lower signal-to-noise ratio  | 15   |
| SAW                           | Real time quantification of cells in 2D and 3D cultures                   | Analyte range is design limited  | 16   |
| QCM                           | Detect very small (nanogram) mass variations                              | Low reproducibility  | 17   |
| Infrared thermography         | Non-invasive, fast imaging time   | Highly prone to false-negative and false-positive results depending on size of tumour and body temperature | 18   |
| DOI/OM                        | Generates 2D and 3D images when combined with other imaging modalities    | Less spatial resolution when used alone  | 19   |
| Microwave-based technique     | Non-ionizing radiation, non-invasive, inexpensive, comfortable            | Not available in clinic or hospital  | 20   |

LFIA: lateral flow immunoassay; SERS: surface enhanced Raman spectroscopy; ELISA: enzyme-linked immunosorbent assay; <sup>1</sup>H-MRS: proton magnetic resonance spectroscopy; EIT: electrical impedance tomography; MEMS: microelectromechanical systems; PMUTs: piezoelectric micromachined ultrasonic transducers; SAW: surface acoustic waves; QCM: quartz crystal microbalance; DOI/OM: diffuse optical imaging/optical mammography.

shown in Fig. 1d and e, indicate that the *ErbB2* free samples form a very small shift (<1 nm) in their resonance wavelength, whereas *ErbB2*-conjugated samples show a wavelength shift of 6 nm. It can be concluded that the device selectively targets *ErbB2* antigen. The results of the study (Fig. 1f) are coinciding in simulation and experiment for

*ErbB2* and anti-*ErbB2* binding. The LOD of the SNP-based biosensor is 0.7 ng mL<sup>-1</sup> with a sensitivity of 2 nm nM<sup>-1</sup> for *ErbB2*. It is also suggested that the lateral flow-through feature, along with optical bound states, supports the increase in the sensitivity of molecule-bond changes in refractive index.<sup>26</sup>

**2.1.2 Flow cytometry.** This lab-based technique measures or counts the cells or particles (in suspension). It comprises a fluidic system and an optical system (lasers), along with a data acquisition system, adjusted with filters and detectors. This system captures fluorescence and scattered signals. The cell sorting and analysis are done on the basis of their fluorescence or light scattering characteristics.<sup>27</sup> This technique is now being commonly used in classifying leukemias and lymphomas. The disproportionate growth and distribution of cells in body, unusual expression of surface receptors, along with tumor antigens, can be characterized by using different flow cytometry-based techniques.<sup>28</sup> Another advancement in flow cytometry has been reported by Bhattacharya *et al.*, in which they employed photoacoustic (PA) flow cytometry to identify circulating BrC cells in human blood. A Q-switched laser, particularly targeting BrC cells having chromophores, is applied to the passing cells and the optically absorbing cells emit an ultrasound wave due to the PA effect. The red curve is characteristic of the presence of only leukocytes, and the blue curve depicts prominent PA

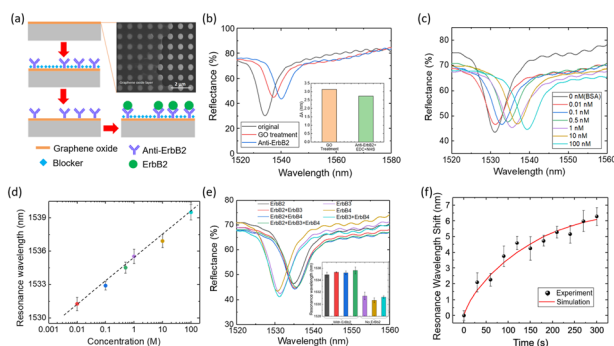


**Fig. 1** (a) Schematic of the label-free assay and SEM of the SNPs. (b) Reflection spectra of the bare sensor, GO layer, and anti-*ErbB2* antibody coating. (c) Reflection spectra in the presence of *ErbB2*. (d) Dose-response curve for the detection of *ErbB2*. (e) Reflection spectra for seven different combinations of *ErbB2*, *ErbB3*, and *ErbB4* antigens. Inset: resonance wavelength in presence of antigens and interfering molecules. (f) Simulation and experimental results for the binding of *ErbB2* and anti-*ErbB2* antibodies. Reproduced from ref. 26 with permission from Elsevier, copyright 2018.



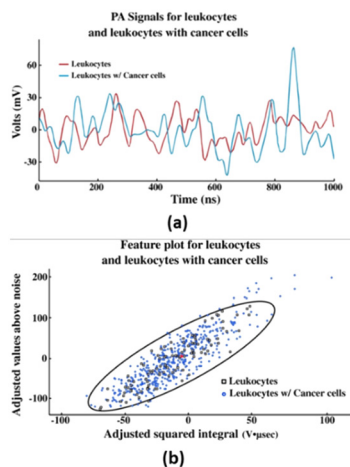


**Fig. 2** (a) PA waveforms obtained from the PAFC test from centrifuged blood. (b) Feature plot of each PA waveform from leukocytes and leukocytes with cancer cells. Reproduced from ref. 29. Published under the terms and conditions of the Creative Commons Attribution 4.0 Unported license.

emission between 850 and 900 ns (Fig. 2a). A plot for PA waveforms obtained during the detection of leukocytes and leukocytes with cancer cells is shown in Fig. 2b. Most of the waveforms are present inside the red boundary and cannot be differentiated from leukocytes. However, towards the top-right, the 17 outliers outside of the red boundary were classified as cancer-containing cells by the automated system. Further, these droplets were captured and imaged to identify separated cancer cells. The features of cells seen at the bottom-left were found to be small and their voltage amount did not present PA signals from cancer cells. Therefore, they are not classified as cancer cells. The study established that the PA flow cytometry can capture single circulating cells with ~43% retrieval rate (25–45 cancer cells per mL blood). The presented method can be employed to govern the disease state of the effected person and their response to the treatment. Further, it can be employed for *in vitro* drug trials and genetic testing.<sup>29</sup>

## 2.2 Optical techniques

**2.2.1 Surface-enhanced Raman spectroscopy (SERS).** SERS is a surface-sensitive, non-destructive vibrational spectroscopy technique that works by identifying the analytes with low concentrations and generating strong electromagnetic fields (“hot spots”), amplifying the scattered signals generated due to the excitation of localized surface plasmons.<sup>30</sup> It presents high sensitivity and specificity and has the ability to detect molecular information from biological samples.<sup>31</sup> Xu *et al.*<sup>30</sup> designed a multiplexed Fe<sub>3</sub>O<sub>4</sub>@CP@SERSnanotag for early and quantitative detection of BrC biomarkers (miRNA: miR-21, miR-155, and let 7b). Fe<sub>3</sub>O<sub>4</sub>@CP@SERSnanotags alone show an increase in Raman signals, whereas, in the presence of biomarkers, the target miRNA specifically

binds with capture probe (CP) and forms DNA/miRNA heteroduplexes. The removal of SERS nanotags from Fe<sub>3</sub>O<sub>4</sub> NPs showed a decrease in the SERS intensity, which is directly related to the amount of target miRNAs. The proposed method presented simultaneous detection of miR-21 (LOD 0.050 fM), miR-155 (LOD 0.063 fM), and let 7b (LOD 0.037 fM).

The authors in ref. 32 report an evaluation of 253 total serum samples from unaffected subjects and patients for differential diagnosis of breast, oral, lung, ovarian, and colorectal cancer. Forty-two patients are diagnosed with BrC using SERS-based detection. The SERS spectra of deproteinized serum were obtained using a 532 nm laser, and the SERS substrates were presented by hydroxylamine-reduced silver nanoparticles (AgNPs). Further estimation was performed using principal component analysis-linear discriminant analysis (PCA-LDA) model for identifying the specific cancer of each sample. The PCA-LDA model depicted 76% efficacy level for BrC. The results indicate that the differential expression of the metabolites in the SERS signal is more profound in breast, ovarian, and oral cancers than that of colorectal and lung cancers. A similar technique has been employed,<sup>33</sup> wherein BrC was diagnosed from the urine sample. For this, urine samples from 53 BrC patients and 22 as control were collected. The SERS spectra were recorded using Ag NPs obtained by reduction with hydroxylamine hydrochloride and further activated with Ca<sup>2+</sup>. This further promoted the adsorption of the anionic purines including uric acid, xanthine and hypoxanthine. By employing PCA-LDA and SERS, the samples from BrC patients were classified with 81% sensitivity and 95% specificity with an overall accuracy of 88%. Both the studies<sup>32,33</sup> suggest the translation of SERS in the clinical setting and emphasize the potential of SERS as a novel and prominent diagnosis strategy for the detection of BrC.

**2.2.2 Enzyme-linked immunosorbent assay (ELISA).** It is the most frequently used immunoassay, which employs enzymatic activity and antibody–enzyme binding as a measure to detect the analytes. The presence of an antigen is detected by the addition of an appropriate substrate, which leads to color change that can be further quantified using a microtiter plate reader. The use of microtiter plate was believed to limit its portability. With the developments in image capturing and processing techniques, it is possible to use ELISA as a point of care device.<sup>34</sup> The paper-based ELISA is an advancement of the conventional ELISA and can be used for diagnostic applications owing to their short analysis time, low cost, and portability, that allows the use of a small quantity of sample. Carneiro *et al.* designed a similar quick, simple and cheaper paper-based colorimetric assay to detect CA15-3 cancer antigen. The linear range of the assay is between 2 and 1100 U mL<sup>-1</sup> in buffer and 2 and 200 U mL<sup>-1</sup> in human serum.<sup>35</sup> Choi and group developed an antibody-lectin sandwich test to detect glycosylation of CA15-3 BrC markers. Glycosylation is considered a sensitive indicator of cancer progression. CA15-3 biomarker is a heavily glycosylated molecule, therefore detecting its glycosylation



can be considered a sensitive approach to measure CA15-3 as compared to the conventional ELISA. In this method, monoclonal antibody anti-CA15-3 serves as a capture antibody and binds with CA15-3 in the serum. The detection of CA15-3 glycosylation is done by concanavalin A (ConA) lectin. The CA15-3 glycosylation reportedly increased with the progression of BrC stages. The technique showed proficient discrimination of BrC stage I (69% specificity, 63% sensitivity), IIA (75% specificity, 77% sensitivity), IIB (86% specificity, 69% sensitivity) and III (65% specificity, 80% sensitivity) from BrC.<sup>36</sup>

**2.2.3 Fluorescence-based methods.** The fluorescence-based methods are an advancement of optical methods, which employ fluorescence dyes and analyze the amount of fluorescence emitted from a contrast agent attached with the specific biomarkers. Lee *et al.*<sup>37</sup> demonstrated the use of pH-based fluorescence lifetime for BrC diagnosis by establishing the relation between fluorescence lifetime and pH using fluorescein. The fluorescence lifetime is the mean time of a molecule, spent in the excited state after absorbing a short-pulsed laser energy. Based on the energy exchange between the fluorophore and its environment, it can be used to obtain biochemical characterization of the cells.<sup>38</sup> Since the normal tissues exhibit a neutral pH, whereas cancer tissues show an acidic pH (due to the release of lactic acid through aerobic metabolic processes), it causes differences in the fluorescence lifetime, which can be used to monitor the progression of cancer. The method further presents a non-invasive technique for real-time, *in vivo*, and *in situ* cancer detection using fluorescence lifetime of the target tissue.<sup>37</sup>

Another work<sup>39</sup> depicts the synthesis of a fluorogenic material functionalized with peptides using self-assembly between molybdenum disulfide (MoS<sub>2</sub>) and a fluorescent peptide probe for fluorescence detection. The developed material presented for the detection of protein C receptor (PROCR), which is a transmembrane biomarker for triple-

negative BrC (TNBC) cells and their imaging. The study used TAMRA (tetramethyl-rhodamine, a fluorescent label) to bind with AN33 (peptide), to form TAMRA-AN33 followed by the synthesis of TAMRA-AN33/MoS<sub>2</sub> composites. To evaluate the fluorescence imaging ability of the synthesized composite, a TNBC cell line MDA-MB-231 (high PROCR expression) and an MCF-7 BrC cell line (low PROCR expression) were used. It was observed that upon increase in TAMRA-AN33 concentration, the fluorescence in MDA-MB-231 cells increased proportionally, whereas, not much change was observed in the fluorescence of MCF-7 cells (Fig. 3a–c). Similarly, upon incubation of TAMRA-AN33/MoS<sub>2</sub>, a fluorescence increment was seen in MDA-MB-231 when MoS<sub>2</sub> concentration was increased up to 20 μg mL<sup>-1</sup>, but MCF-7 cells remained unaffected (Fig. 3d and e). This indicates that MoS<sub>2</sub> enhances the peptide probe binding with the membrane-bound PROCR by clustering effects.<sup>40</sup> Additionally, the cell proliferation assay suggested good compatibility of the peptide probe for pharmacological investigations. The targeting capability of the composite was also investigated and it presented with a strong imaging signature for the BrC cells.

#### 2.2.4 Proton magnetic resonance spectroscopy (<sup>1</sup>H-MRS).

The malignant cancer cells show increased proliferative activity, leading to changes in the cell membrane metabolism and subsequently increasing the choline levels that serve as image-based cancer biomarkers.<sup>41</sup> <sup>1</sup>H-MRS is used to measure the resonance of protons to generate a spectrum, which assists in the identification of BrC biomarkers. A systematic review and metanalysis reports mention the use of tCho as diagnostic biomarkers for BrC detection. The specificity and sensitivity of <sup>1</sup>H-MRS are found to be 78–80% and 71–74%, respectively.<sup>42</sup> Another systematic review based on 159 studies and 26 papers confirmed that the metabolic concentrations obtained using <sup>1</sup>H-MRS can be related to the diagnosis and treatment response in BrC patients.<sup>43</sup> MRS-

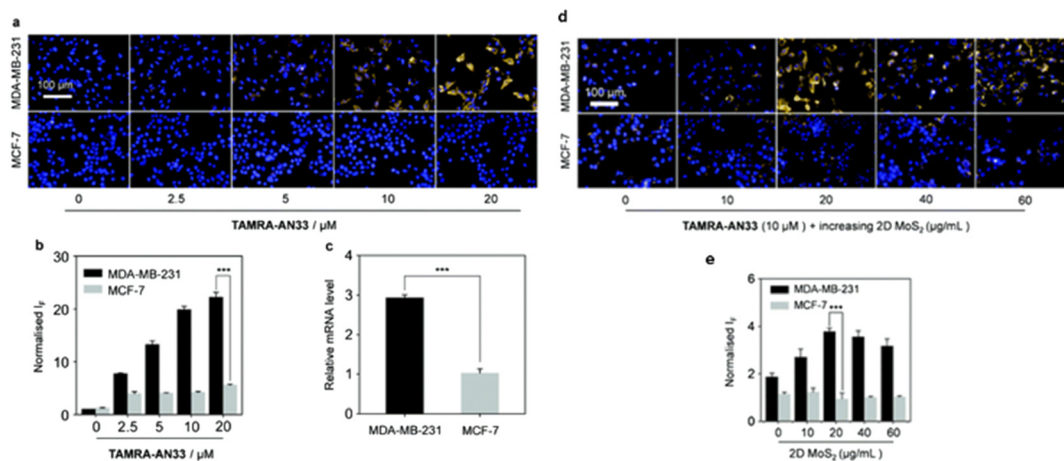


**Fig. 3** (a) Fluorescence imaging, (b) quantification of MDA-MB-231 and MCF-7 cell lines treated with TAMRA-AN33, (c) relative mRNA level of PROCR in MDA-MB-231 and MCF-7 cells using RT-qPCR method, (d) fluorescence imaging, and (e) quantification of MDA-MB-231 and MCF-7 treated with TAMRA-AN33 and MoS<sub>2</sub>. Reproduced from ref. 39. Published under the terms and conditions of the Creative Commons Attribution 3.0 Unported license.



based lipid profiling may provide a multivariate approach for BrC characterization. MRS spectra, through the stimulated echo acquisition mode sequence, were obtained from patients. Fat peaks were quantified using the LCModel software. The results presented that the mean concentrations of all lipid metabolites and PUFA were much lower in tumor cells ( $p \leq 0.002$ ) than the normal tissue ( $p \leq 0.04$ ). Similar results were observed in case of HER2-positive vs. HER2-negative tumors.<sup>44</sup> A study to establish the diagnostic accuracy of MRS in breast lesions was conducted, in which 159 diagnosed patients underwent <sup>1</sup>H-MRS using a 1.5 Tesla MR system and fast scans in multiple planes were produced. It was concluded that <sup>1</sup>H-MRS is a reliable diagnostic technique for malignant breast lesions and can be employed as an efficient early detection tool for risk-prone age groups.<sup>45</sup>

### 2.3 Electrical techniques

Electrical impedance tomography (EIT) also known as electrical impedance scanning is used to estimate various electrical properties of breast tissue. It is a method where there is no or zero exposure to any form of radiation, and the breast tissue can be safely examined without facing any hazardous conditions.<sup>46</sup> This is completely a non-invasive and user-friendly method with facilities of mobile screening. The mechanism followed by this method is the measurement of impedances using dense electrodes to be placed on the surface of the patient's body. The result is further generated as reconstructed tomographic images, 2D or 3D. Here, impedance mainly involves both conductivity and/or permittivity, and as it changes, the EIT imaging starts its activity. The important mechanisms it follows are data acquisition and image reconstruction.<sup>47</sup>

Lee *et al.*<sup>48</sup> designed and proposed an 8-channel 10 MHz wide bandwidth EIT-AFE-IC having a wide dynamic range, reconfigurable front-end architecture, and a phase compensation loop for high precision detection of BrC. This wide bandwidth EIT system could go up to 10 MHz and portrayed a small phase error of 4.32 degree and could detect an object of 0.5 cm. The results were confirmed using phantom experiments.

A mobile-based EIT demonstrated by Hong *et al.* has a brassiere shape and EIT IC is integrated using a fabric-based board, which consists of an EIT electrode array, electronic circuitry and imaging device.<sup>49</sup> This IC has a chip size of 0.18  $\mu\text{m}$  size 1P6M CMOS process with a consumption of 53.4 mW. The system offers 4.9 m $\Omega$  sensitivity and detects a 5 mm cancer mass (0.1% breast volume) within an agar test phantom. The complete time taken for EIT measurement is less than 10 s. in a recent study by Wan *et al.*,<sup>50</sup> HER2 and CA15-3 biomarkers were included into commercially accessible disposable strips, which are functionalized to detect BrC. These strips resemble the widely used glucose detection strips. The findings showed that the limits of detection for these two biomarkers were as low as 1 fg mL<sup>-1</sup>,

which is significantly lower than the range of 1–4 ng mL<sup>-1</sup> for the traditional enzyme-linked immunosorbent test. The detected signal was obtained by applying 10 1.2 ms voltage pulses to the transistor's drain electrode and sensing strip electrode using a synchronized double-pulse method. The average of the 10 digital output readings that corresponded to those 10 voltage pulses was the detected signal. For HER2 and CA15-3, the sensor sensitivity values were attained at about 70/dec and 30/dec, respectively.

### 2.4 Electrochemical techniques

Electrochemical sensors are simple, sensitive, and cost-effective devices for cancer detection. The electrochemical techniques detect the change in electrochemical parameters such as resistivity, current, and redox reactions at the electrode and interpret them for diagnostic results.<sup>51</sup> Zare *et al.*<sup>52</sup> report the synthesis of an electrochemical biosensor showing prominent electrochemical activity, porosity, and dispersity, along with a large surface area for better functionalization. The biosensor is made of a haemoglobin-capped Ag nanocluster conjugated with a Cu(II)-porphyrin-metal organic framework in a graphene-incorporated nanohybrid probe. The Hb-AgNCs@MOF-G nanocomposite immobilizes anti-HER2 on a glassy carbon electrode to detect the presence of HER2-positive BrC cells using electrochemical impedance spectroscopy (EIS) “signal on” and square wave voltammetry (SWV) “signal off” techniques. It reportedly detects 2 cells per mL using EIS “signal on” and 16 cells per mL by SWV “signal off”. The sensor demonstrates 15–16 fold selectivity with a recovery efficiency in the range of 94.8 to 106% by the EIS method and 95.4 to 111% *via* the SWV method.

Another multiplexed electrochemical biosensor has been fabricated using screen-printed carbon electrodes functionalized with gold nanoparticles in conjugation with graphene quantum dots and graphene oxide (AuNPs/GQDs/GO) to detect BrC-related microRNAs (miRNA-21, miRNA-155, and miRNA-210). It further involves the use of anthraquinone, methylene blue, and polydopamine as redox indicators, which hybridize with the complementary targets, miRNA-21, miRNA-155, and miRNA-210, respectively. The qualitative and quantitative estimation of each miRNA is identified by its respective peaks and their intensity. The developed biosensor demonstrated efficient sensing of miRNA. It renders a wide linear range of 0.001–1000 pM with low detection limits of 0.04 (miRNA-21), 0.33 (miRNA-155), and 0.28 fM (miRNA-210).<sup>53</sup>

A similar electrochemical sensor has been demonstrated using a GO-IL-AuNP (graphene oxide-ionic liquid-gold nanoparticles) hybrid nanocomposite on a glassy carbon electrode to detect the presence of a BrC biomarker, CD44 antigen. The functionalization of IL with GO helped in tremendously increasing the conductivity of GO. The biocompatibility of IL augments the loading capacity of the anti-CD44 molecule and prohibits the lumping of the



**Table 2** Electrochemical diagnostics for BrC with parameters included

| Biomarker | Technique                                    | Transducer       | LOD                                     | LR   | Sensitivity                  | Ref. |
|-----------|--|------------------|---|--|------------------------------|------|
| HER2      | Differential pulse voltammetry (DPV)         | 8 × SPE          | 1.8–2.6 ng mL <sup>-1</sup>             | 0–20 ng mL <sup>-1</sup>                                     | Validated                    | 55   |
|           |  | AuE              | 0.995 pg mL <sup>-1</sup>               | 0.01–10 ng mL <sup>-1</sup> ,<br>10–100 ng mL <sup>-1</sup>  | 5.921 μA mL ng <sup>-1</sup> | 56   |
|           |  | SPCE             | 6.0 ng mL <sup>-1</sup>                 | 0–30 ng mL <sup>-1</sup>                                     | 6 ng mL <sup>-1</sup>        | 57   |
|           | Electrochemical impedance spectroscopy (EIS) | Au@PdAg DBNR/GCE | 0.25 pg mL <sup>-1</sup>                | —  | —                            | 58   |
|           |  | CILE             | 7.4 ng mL <sup>-1</sup>                 | 10–110 ng mL <sup>-1</sup>                                   | Validated                    | 59   |
|           |  | GSPE             | 6.0 μg mL <sup>-1</sup>                 | 0–40 μg mL <sup>-1</sup>                                     | —                            | 60   |
|           |  | Au/AuNP          | 5.0 ng mL <sup>-1</sup>                 | 10 <sup>-5</sup> –10 <sup>2</sup> ng mL <sup>-1</sup>        | —                            | 61   |
|           | Linear sweep voltammetry (LSV)               | IDμEs            | 1 pM L <sup>-1</sup>                    | 1 pM–100 nM  | 0.035 μF/log([HER2] pM)      | 62   |
|           |  | SPCE             | 4.4 ng mL <sup>-1</sup>                 | 15–100 ng mL <sup>-1</sup>                                   | —                            | 63   |
|           | Amperometry                                  | SPCE             | 1.0 μg mL <sup>-1</sup>                 | 1–200 μg mL <sup>-1</sup>                                    | —                            | 64   |
| DPV       |  | GCE              | 0.015 U mL <sup>-1</sup>                | 2.0–25.0 U mL <sup>-1</sup> ,<br>0.05–2.0 U mL <sup>-1</sup> | —                            | 65   |
| CA15-3    | Cyclic voltammetry (CV)                      | GCE              | 0.012 U mL <sup>-1</sup>                | 0.1–20 U mL <sup>-1</sup>                                    | —                            | 66   |
|           |  | AuE              | 5 × 10 <sup>-6</sup> U mL <sup>-1</sup> | 2 × 10 <sup>-5</sup> –40 U mL <sup>-1</sup>                  | —                            | 67   |
|           |  | AuE              | 0.040 U mL <sup>-1</sup>                | 0.1–160 U mL <sup>-1</sup>                                   | —                            | 68   |
|           | DPV  | AuE              | 0.640 U mL <sup>-1</sup>                | 2.0–240 U mL <sup>-1</sup>                                   | —                            | 69   |
|           |  | AuE              | 0.6 ng mL <sup>-1</sup>                 | 1.0–240 ng mL <sup>-1</sup>                                  | —                            | 70   |

8 × SPE: eight screen-printed electrochemical cells, AuE: gold electrode, AuNPs: gold nanoparticles, Au@PdAg DBNR: Au@PdAg dog-bone-like nanorod, CILE: carbon ionic liquid electrode, CV: cyclic voltammetry, DPV: differential pulse voltammetry, EIS: electrochemical impedance spectroscopy, GCE: glassy carbon electrode, GSPE: graphite screen-printed electrode, HER2: human epidermal growth factor receptor, IDμEs: interdigitated gold micro-electrode arrays on silicon/silicon oxide wafers, LOD: limit of detection, LR: linear range, LSV: linear sweep voltammetry, SPCE: screen-printed carbon electrode.

nanocomposite materials improving their stability. The AuNPs in the nanocomposite increase the surface area, which favors the immobilization of anti-CD44 antibodies, and also improve the conductivity of the nanocomposite. All the components result in the synthesis of a highly specific and sensitive device for CD44 detection with a wide range of detection of 5.0 fg mL<sup>-1</sup> to 50.0 μg mL<sup>-1</sup> and an LOD of 2.80 fg mL<sup>-1</sup>.<sup>54</sup> Table 2 summarizes a few electrochemical diagnostics for BrC with respect to the biomarkers, techniques and quantifiable parameters.

Bioimpedance is an electrochemical-based technique in which current is passed to the object through electrodes, and the electrical impedance generated gives an impedance score based on its electrical characteristics. The impedance value can be used to differentiate between cancerous (low impedance) and normal tissues (higher impedance).<sup>71</sup> In the study by Mansouri and group,<sup>72</sup> a low-frequency current of 1 kHz, 0.9 mA is introduced through a device to measure the differences in the extracellular resistance (from 0.6 g l<sup>-1</sup>) between the breasts. It is suggested to visit the doctor if the difference is more than 50 Ω. The breast afflicted by the cancer can be determined by looking at the resistance with the lowest value.

## 2.5 Breath-based techniques

BrC can alter the metabolic constitution and synthesis of volatile metabolites in the breath of patients, which can serve as a non-invasive diagnostic marker. The ER, PR and HER2 biomarker receptors exhibit unique metabolomic expression in BrC patients.<sup>73</sup> There are different methods to identify breath VOCs. One is traditional, GC-MS, and the other is

advanced, electronic nose. The latter uses an array of sensors and machine learning algorithm to map the breath print to breath VOCs.<sup>74</sup> Types of breath tests for BrC analysis have been presented by Yang *et al.*<sup>75</sup> based on volatile compounds found in the exhaled alveolar breath, with an electronic nose (E-nose) made of an array of carbon nanotube sensors. The volatile organic compounds (VOCs) interact with the array and generate a change in their electric resistance. Further, machine learning was employed to create prediction models for BrC detection and its molecular phenotyping. The breath samples were analyzed using HPPI-TOFMS (high-pressure photon ionization-time-of-flight mass spectrometry). The E-nose system can execute rapid breath biopsy, (in 30 min), which generally requires 7 days. The test reports 86% sensitivity, 97% specificity, and 91% prediction accuracy using the random forest model for 899 volunteers. Another study was conducted on 5047 women based on VOC markers, wherein 465 (9.21%) participants were identified with BrC. It employed similar breathomics and forest algorithm techniques, as reported in the previous study. The results indicated 96.97% detection rates and 87.70% specificity for ductal carcinoma.<sup>76</sup>

The profiling of BrC with 276 subjects using VOCs is portrayed<sup>77</sup> in Fig. 4, wherein the breath analysis was done by GC-MS and nanoarray technology. Twenty-three compounds including alkanes, methylated alkanes, chlorinated alkanes, ethers aldehydes, alcohols, ketones, acetic acid and benzene derivatives were identified as belonging to various molecular sub-types of BrC. These VOCs were found similar to the previously reported results of breast-derived cell lines.<sup>78</sup> Particularly, 2-ethyl-1-hexanol was identified as a potential biomarker for BrC progression.



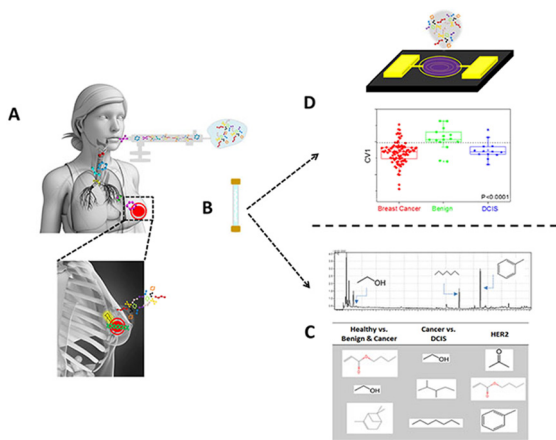


**Fig. 4** (A) Patient exhales into a collection bag. (B) Collection and concentration of breath on Tenax® (C) exposure of the Tenax® tube to GC-MS for detecting the presence of specific compounds. (D) Exposure to the AI nanoarray for volatolomic signature of BrC genetic mutations. Reproduced from ref. 77 published under the terms and conditions of the Creative Commons Attribution license.

Furthermore, certain VOCs were found to be the products of DNA damage caused by the action of reactive oxygen species (ROS) present in tumor cells. ROS also induces the upregulation of cytochrome p-450 enzyme, which further leads to the peroxidation of polyunsaturated fatty acids in the cell membranes. This results in the overexpression of volatile alkanes and alkane-derivatives in the breath.<sup>79</sup> The discriminant function analysis (DFA) of the nanoarray recognized specific differences in the volatolomics between affected and non-affected cells, and different molecular subtypes with 82–87% accuracy, 76–96% specificity and 81–88% sensitivity. Another work presented by Herman-Saffar *et al.* demonstrated that commercial electronic noses and GC-MS can be used to detect initial stages of BrC. They processed exhaled breath samples from 48 BrC patients and followed artificial neural networks for statistical analysis. The model showed up to 95.2% accuracy for the classification of BrC patients.<sup>80</sup> In another study, 443 exhaled breath samples, having 262 diagnosed with BrC, were collected. The results indicated that the breath prints of BrC patients differed from those of healthy women, with a valid classification rate of 98% and a range up to 98.8%. The ROC curve indicates that the sensitivity, specificity, negative predictive value, and positive predictive value were all 100%. This study shows that the electronic nose can distinguish between BrC patients and healthy individuals.<sup>81</sup>

## 2.6 Mechanical techniques

**2.6.1 Microelectromechanical systems (MEMS).** MEMS consist of an electrical and a mechanical component combinedly working as sensors, and can be used to analyze samples at the micro scale.<sup>82</sup> The changes in the biophysical parameters of breast tissues during the progression of tumors can assist as a label-free marker to distinguish

tumors from unaffected tissues. On a microscale level, these transformations are imitated as changes in thermal, electrical, and mechanical responses which can render a more objective assessment. One such MEMS-based study<sup>83</sup> presents a conjugation of an electrothermal sensor on a microchip, equipped with a mechatronic actuation system, along with a graphical user interface. The developed sensor provides quantitative information of the thermal conductivity, and also bulk and surface resistivities of the sample. A high value of surface resistivity indicates high surface irregularity and poor conformability, which is present in the cancerous tissue.<sup>84</sup> The cancer infected tissues are stiffer than normal tissues, which make them less conformal to the microchip surface. They also have a higher volume of temperature sensitive collagen fibers, which further cause an increase in resistivity.<sup>85,86</sup>

Khosla<sup>87</sup> has presented a novel nano electrode array-based electroimpedance tomography for non-invasive and radiation-free medical imaging. It has been reported as the first device employing a nano-electrode array integrated to a flexible textile sensor fabricated using MEMS. It can scan through a wide range of frequencies and allow for simultaneous scanning of both the breasts. Further, it is reported as the first sensor that parallelly scans lymph nodes present under the arm. These features can assist in tracking cancer progression and treatment.

A RapidET:MEMS-based platform has been evidenced that can quickly demarcate between normal breast and biopsy tissue. The technique is label free and the microchip is based on electrothermal sensing. This MEMS platform contains a platinum microheater, interdigitated electrodes (IDEs), and resistance temperature detectors (RTDs). Fig. 5a depicts the design of the microchip with other elements fabricated on a SiO<sub>2</sub> wafer. The optical photograph and SEM are shown in Fig. 5b and c, respectively. A thermal isolation trench of 350 μm depth was designed around the microheater for maintaining a uniform temperature around the microheater. This also reduces the temperature dissipation to other elements such as RTDs. This trench was first simulated in COMSOL to assess its effects.<sup>88</sup> Fig. 5d displays the sample holder that comes into contact with the sensor holder (Fig. 5e). The detailed picture of the sample holder is shown in Fig. 5f, and the enlarged image of microchip is shown in Fig. 5g and h.

The parameters bulk resistivity, surface resistivity and thermal conductivity were measured, and a pathologist confirmed whether the tissue is normal or tumorous. The biopsy tissues were deparaffinized formalin-fixed paraffin-embedded (FFPE) tissues and formalin-fixed fresh tissues. Using this RapidET system, the microheater provided different temperatures to the tissues and both bulk ( $\rho_B$ ) and surface resistivity ( $\rho_S$ ) were measured.

It was observed that both these values were higher for tumor tissues at higher temperatures. A similar trend was found for both formalin fixed and deparaffinized tissue samples. The mean  $\rho_B$  was measured to be 4-fold for tumor



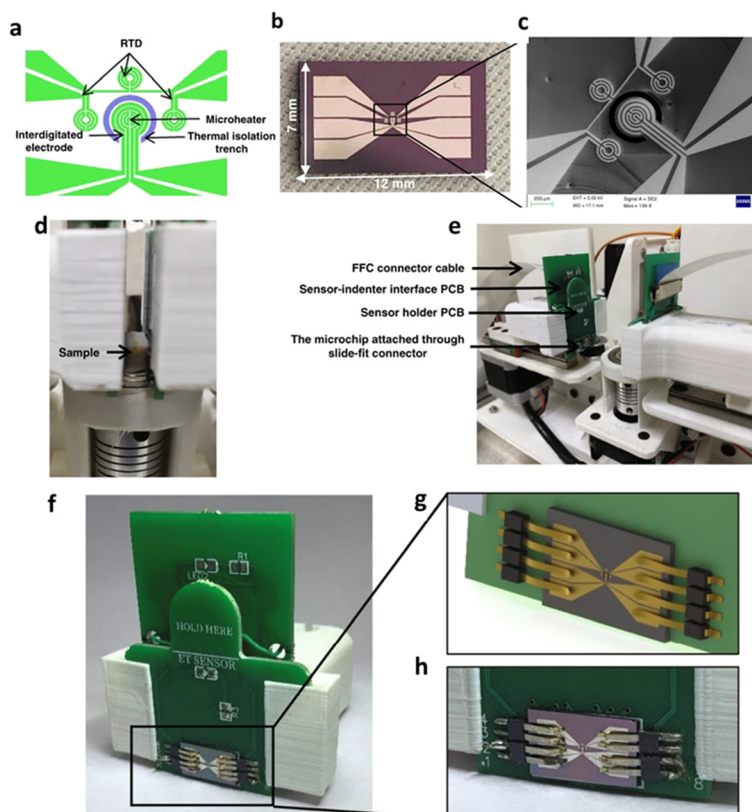


**Fig. 5** (a) Microchip design, (b) optical photograph of the fabricated microchip, (c) SEM image of the active area of the microchip, (d) sample loaded in the system, (e) subsystem with the PCBs, (f) microchip packaged into the sensor holder structure through slide-fit contacts, (g and h) rendered and actual image of the microchip connected to the slide-fit contacts. Reproduced from ref. 88 published under the terms and conditions of Creative Commons Attribution 4.0 International license.

tissues in comparison to the 3-fold change in case of normal tissues. A lower thermal conductivity ( $K$ ) was exhibited by tumor tissues than normal tissues. The mean  $K$  of the formalin-fixed tumor tissues was a smaller value of  $0.309 \pm 0.02 \text{ W m}^{-1} \text{ K}^{-1}$  compared to  $K$  of  $0.563 \pm 0.028 \text{ W m}^{-1} \text{ K}^{-1}$  of normal tissues. Further fisher's combined probability test and regression analysis asserted that these three parameters play a key role in identifying tumor tissues from BrC patients.

Palpreast is a wearable device that is specially designed to imitate the process of breast self-examination in women for the detection of cancer. The device is non-invasive and uses pressure-sensing-based textiles and further enhances confidence and self-awareness among women. The device is based on large- and medium-sized breast phantoms. It mimics the exact function of a human hand. The textile pressure sensor and the inflator system, as shown in Fig. 6, are embedded inside the smart top or fabrics used by women, and it protects the entire breast. To avoid any excessive expansion of the inflator, the smart wearable device consists of an internal pocket. The inflator system has a bulb pump with an air release valve, and a manometer to verify the pressure, along with properly designed T-valve structures to balance the air flux present in each compartment, as a result of which balloons inserted in each compartment layer

inter-connected to the pumping system through rubber hoses are inflated.<sup>89</sup>

**2.6.2 Piezoelectric micromachined ultrasonic transducers (PMUTs).** These are extensions of MEMS devices, which assist in *ex vivo* characterization of breasts using single cells, tissue sections, and whole tissues. PMUTs show better sensitivity in differentiating normal cells from cancerous cells by assessing



**Fig. 6** Prototype design of the Palpreast device, including a smart wearable and inflator system. Reproduced from ref. 89 published under the terms and conditions of the Creative Commons Attribution (CC BY) license.



the vascular density, mechanical stiffness, acoustic impedance, and viscoelastic parameters.<sup>90</sup> Further, such devices are associated with microneedles equipped with tissue-specific targeting for the surgical removal of cancers.<sup>91</sup> A 3D ultrasound imaging ring system using a PMUT linear array has been designed with a circular scanning method for BrC detection. This setup can provide 3D scanning of the breasts along with the identification of the size, location, and outline of the cancerous tissue. The  $1 \times 128$  PMUT linear array is placed at  $90^\circ$  in a cross-vertical manner and the transducer surrounds the mammary gland, facilitating a non-contact detection.<sup>92</sup>

**2.6.3 Surface acoustic waves (SAWs).** They detect targeted cells or tissues in a fluid or solid state by using mass loading on acoustic-wave devices. SA waves are produced at the piezoelectric material surface by applying voltage to the metal interdigital transducer (IDT). Such waves travel through the delay line region to reach the IDT output and cause a mechanical shift, which further creates a voltage difference. Any modification in the device surface by selective coatings can be done to deploy mass loading. The interaction of the functionalized device surface with the entity being sensed creates changes in the resonant frequency, which are further measured to analyze the sample. SAW sensors in combination with complementary metal-oxide semiconductor (CMOS) has been employed to detect hMAM, a BrC biomarker, using streptavidin/biotin-based immunoassay. It can detect BrC biomarkers at low cost, higher sensitivity and enhanced repeatability of fabrication. Chang and co-workers developed another such method for detecting BrC using a novel  $2 \times 3$  model of a leaky surface acoustic wave (LSAW) aptasensor array. The aptamer was assembled on a gold electrode surface of 100 MHz LiTaO<sub>3</sub> piezoelectric crystal. The interactions between the aptamer and MUC1 protein expression on the cancer cell surface could successfully capture the MCF-7 cells. The aptamer-cell complex amplified the mass loading capacity of the LSAW sensor.<sup>93</sup> In another study, an ultra-miniaturized microfluidic chip using a narrow-path travelling surface acoustic wave (np-TSAW) has been made for the isolation and purification of BrC cells (MCF-7) from blood with 98% isolation efficiency and 93% purity.<sup>94</sup>

**2.6.4 Quartz crystal microbalance (QCM).** QCM is a piezoelectric sensor in which the mass loaded on the sensor causes a shift in the resonator oscillation frequency. The interactions between the surface immobilized biomolecules can be studied by measuring the frequency shift of the resonator.<sup>95</sup> This phenomenon has been employed to detect the changes in cell surfaces of BrC cells such as over expression of Notch-4 receptors. The techniques involve the development of QCM biosensors conjugated with PHEMA-NPs (poly(2-hydroxyethyl methacrylate) nanoparticles) further functionalized with a Notch-4 receptor antibody. It detected MDA-MB-231 cells with a detection limit of 12 cells per mL.<sup>96</sup> Another such QCM-based biosensor coated with hydroxyethylmethacrylate (HEMA) and ethylene glycol

dimethacrylate (EDMA) polymeric nanoparticles and modified with an HER2/neu antibody has been synthesized with a detection limit of 10 cells per mL. SKBR3 cells were taken for the expression study.<sup>97</sup> QCM biosensors are highly sensitive, rapid, reusable, and cost-effective biosensors for cancer cell detection.

## 2.7 Thermal-based technique (infrared thermography)

It is a non-invasive technique that creates a series of infrared scans of the breasts by mapping the temperature difference. The temperature of the tumor tissue is different from that of the non-cancerous tissue, and this difference is generated as a particular thermographic pattern, which can be analyzed for disease characterization. The physiologic image obtained from infrared imaging is in sync with the anatomic image created through mammography, with a very high sensitivity and a negative predictive value. The scans of IR thermography can be additionally used for ensuring the presence of a breast abnormality seen in mammograph.<sup>98</sup> The images are further analyzed by computer algorithms to compare the infrared patterns. It can also assist in differentiating the benign or malignant nature of the lesion.<sup>99</sup> Ekici and Jawzal<sup>100</sup> developed an algorithm for early detection of BrC using image-processing techniques for analyzing thermal breast images. The proposed algorithm is based on convolutional neural networks optimized by Bayes algorithm with an accuracy rate of 98.95%. Likewise, Resmini *et al.*<sup>101</sup> used genetic algorithms and support vector machine for early diagnosis of BrC using infrared thermography with 97.18% of accuracy and 94.79% area under the receiver operating characteristic curve.<sup>86</sup> Another extensive work describes a system that produces thermographic images of breast and further characterizes them as cancerous and non-cancerous. The study suggests that a combination of gradient vector flow and convolutional neural network can detect BrC using the thermographic image characterization.<sup>102</sup>

## 2.8 Imaging technique

It is a lesion detection technique based on functional abnormalities using near-infra-red light, evidenced to detect up to 85% lesions. The breast lesions are identified on the basis of increased hemoglobin concentration and reduced oxygen saturation, which are related to the increased vascularization of tumor cells. DOI techniques include *Transillumination*, which creates 2D images, and diffuse optical tomography (DOT), which generates 3D images.<sup>103</sup> A digital breast tomosynthesis (DBT)/DOT fusion imaging for initial diagnosis of BrC on 28 women has been explored. The receiver operating characteristic curves showed significant improvement, and the technical success rate was 96.4%.<sup>104</sup> Diffuse optical tomography breast imaging system (DOTBIS) non-invasively measures hemoglobin concentration, which is a potential biomarker for short-term response to neoadjuvant chemotherapy. The study conducted by McGuinness<sup>105</sup> analyzed 7 postmenopausal



women with stage I-III BrC enrolled in pre-surgical studies and performed DOTBIS pre- and post-therapy in the affected and unaffected breast. It was observed that DOTBIS-derived observations are modifiable with pre-surgical targeted therapies. The findings support DOTBIS as a potential imaging tool for assessing neoadjuvant targeted therapies in early-stage BrC. Further, to explore the clinical applicability of the diffuse optical inspection device, a compact multi-wavelength DOT system for breast imaging with a fiber-free parallel-plane structure is developed for acquiring the 3D optical properties of the breast.<sup>106</sup>

### 2.9 Microwave-based technique

Microwave-based diagnostics for BrC offers a pain-free method with less scanning time and cost effectiveness.<sup>107</sup> These can be classified into wearable, RF and imaging (radar and tomography). This technique is a contrast to the electrical method, wherein sensors sense the change in signal passing through waveguides, transmission lines lumped capacitors, *etc.*, against the mass/temperature of the tissues.<sup>108</sup>

A fully textile antenna-based detection system envisioned as “smart bra”, which can be worn on the breasts with dimensions  $24 \times 45 \times 0.17 \text{ mm}^3$ , has been presented.<sup>107</sup> An impedance bandwidth from 1.6 GHz up to 10 GHz at  $|S_{11}| \leq -6 \text{ dB}$  ( $\text{VSWR} \leq 3$ ) and from 1.8 to 2.4 GHz and from 4 up to 10 GHz at  $|S_{11}| \leq -10 \text{ dB}$  ( $\text{VSWR} \leq 2$ ) has been realized. The authors also used machine learning algorithms to classify different scanning states using recorded  $S$  parameters. In the imaging process, the antenna sends signals to the breasts and receives the backscattered signals.<sup>109</sup> Islam *et al.*<sup>110</sup> developed a small-side slotted antenna for the microwave imaging of the breast tumor. A heterogeneous breast phantom has been synthesized to simulate the human breast, and it contained the same dielectric properties as those of humans. Since the tumor cells have a higher water content than that of the healthy ones, the dielectric value of the tumor cells is also very high. This caused a change in the backscattered signals received from both tumor and healthy cells. The system consisted of a  $1 \times 9$  antenna array with an RF switching system to control the receivers, signal processing and image reconstruction unit. The collected back scattered signals were processed using the iteratively corrected delay and sum imaging algorithm, which reconstructed the image of the breast interior for multiple tumor sensing.

A clinical prototype as a wearable device for breast health monitoring comprising 16 flexible monopole antennas embedded in a bra has been developed.<sup>111</sup> The data received from this prototype were compared with the table-top version. It works on the principle of multistatic radar. A small pulse is generated, amplified and transmitted through a switching matrix to a transmitting antenna. A 16-element wideband antenna array surrounds the breast under test. The back scattered waves received from the breasts after the

waves pass through the breasts are received at 15 receiving antennas. A picoscope was employed for collecting and storing data. The wearable prototype has reduced the uncertainties by improvement in the fixed positioning of breast and the collection of stronger signal levels, leading to a high signal-to-noise ratio. Since wearables can be directly worn, they reduce the chances of offset error, which is caused in the table-top version due to an additional medium required.

## 3. Commercially available solutions for cancer detection

### 3.1 Blue box device

The blue box<sup>112</sup> is an electronic nose containing chemical sensors that detect BrC biomarkers present in the urine samples. It is a test at-home BrC detection device. Designed with an integrated artificial intelligence (AI) algorithm along with sophisticated technologies, it is used to trace late-stage BrC. There are in total 6 chemical sensors placed inside the box. Within 30 minutes of sample collection, one can know results on the user's phone through an app. In terms of accuracy, the device produces an excellent result of 95%. It renders non-irradiating, painless, and low-cost diagnosis along with a simple and in-home BrC screening. It offers a sensitivity of 88%, an accuracy of 83% and a specificity of 75%.

### 3.2 Human BrC BRCA1 protein ELISA kit

MBS008497 from MyBioSource<sup>113</sup> is a hassle-free ready-to-use strip plate with an ELISA kit to identify the presence of the BRCA1 target analytes in the biological samples. The kit concentration gradient and positive controls offer a detection range in biological samples containing BRCA1. The kit follows the quantitative sandwich-immunoassay procedure. The MBS008497 kit exploits the BRCA1 antibody-BRCA1 antigen interaction (immunosorbent) along with an HRP-conjugated colorimetric detection system to identify BRCA1. It has a detection range as  $0.625\text{--}20 \text{ ng mL}^{-1}$  with a sensitivity of  $0.1 \text{ ng mL}^{-1}$ .

### 3.3 Human cancer antigen CA15-3 ELISA kit

Human cancer antigen CA15-3 ELISA kit (ab108633\_abcam)<sup>114</sup> is another product intended to quantitatively measure the concentration of CA15-3 protein in the human serum sample. In patients with breast tumors, there is an elevated amount of CA15-3 (*i.e.* 25% more) concentrations being estimated (the normal concentration of CA15-3 usually ranges up to 30 units per mL). This protein is mostly shredded by the tumor cells into the bloodstream and acts as a disease-specific tumor marker. Using this kit, the minimum detectable concentration of CA15-3 is estimated to be  $5 \text{ U mL}^{-1}$ .



### 3.4 HercepTest kits

HercepTest is an FDA-approved semi-quantitative immunohistochemical assay for the recognition of HER2 proteins that are overexpressed in BrC-associated tissues.<sup>115</sup> The kit comprises various reagents needed for the immunohistochemical staining. The HercepTest™ is interpreted as negative for Her2 protein at 0 and 1± score, equivocal at 2+ score, and positive for 3± score.

### 3.5 Xpert® BrC STRAT4

The Xpert® BrC STRAT4<sup>116</sup> test kit provides an accurate, standardized, and reliable biomarker for the qualitative estimation of ER, PR, HER2, and Ki-67 mRNA within 2 hours. This strip follows the semi-quantitative method for the detection of biomarkers in the case of invasive BrC. The method involves robust testing and workflow that does not need any PCR laboratory testing.

## 4. Implantable devices for BrC detection

In recent times, medical devices in the form of *in vivo* sensors and therapeutics have played an important role in the early diagnosis and treatment. The traditional hospital-centered diagnostic process and monitoring is now moving towards patient-centered monitoring. Such type of remote healthcare monitoring needs reliable and affordable solutions. Thus, automated biomedical devices are being developed to address the needs of patients. In this context, implantable devices, which are electronic devices used in medical field, have played a key role. The research is, however, also shifting towards biodegradable implantable devices that degrade harmlessly in the human body and work in the human system without being rejected by the patient's immune response. This, further, rules out the dependency of battery and surgical removal after use which imposes a financial load and severe pain on patients. Triboelectric nanogenerators, which utilize mechanical energy and further transform it into electricity, are also new-age biodegradable implantable devices, showcasing massive potential in cancer therapeutics.<sup>117,118</sup>

An implantable device capable of detecting a BrC biomarker (lactate) has been reported by Gil and his team.<sup>119</sup> The device has demonstrated high sensitivity, a pH less than 0.1 (4.2 mV potential) and 1 mM lactate (70 nA current) level. It can operate at distances of 50 mm (10 μW) as tested inside an anatomical model of the human breast. Such safe and specific devices are highly beneficial for BrC screening and provide real-time access to intrabody tissue monitoring post-surgery. This simultaneously assists in assessing the healing or development of any infection in the tissue.

A microporous poly(ε-caprolactone) (PCL) scaffold has been developed as an implant that can identify metastatic BrC cells at early stage. The number of immune cells at the PCL scaffold, which had stabilized prior to tumor

inoculation, altered after tumor inoculation. This scaffold can be used in combination with label-free imaging of early stage metastatic cells, or implanted in patients for monitoring and scheduling follow-up visits using the optical imaging technique.<sup>120</sup>

A multifunctional implantable anticancer device has been fabricated for postsurgical BrC treatment. It is a nanocomposite made of iron oxide nanoparticles, graphene oxide and doxorubicin in a nanofiber matrix that enables target-specific and sustained drug release over 60 days *in vitro*. It has shown significant results in eradicating the local regional recurrence of BrC. Additionally, it reportedly helps in breast reconstruction post-surgery *via* the adipogenic process. The implantable scaffold exhibits enhanced specificity with real-time monitoring and long-term anticancer efficacy.<sup>121</sup>

## 5. Future diagnostics and key challenges for BrC detection

The Internet of Things (IoT) has emerged as a novel and progressive way in the last decade, providing a way for real-time as well as past data analysis. With the use of artificial intelligence (AI), wireless sensor network (WSN), and machine learning (ML), it has advanced rapidly into medical diagnostics. AI and ML tools render enhanced computer-aided diagnosis, medical image processing, interpretation, retrieval, and analysis with add ons of predicting diseases, thus aiding to early diagnosis.<sup>122</sup> Onasanya and Elshakankiri<sup>123</sup> proposed an IoT-enabled system for enhanced detection, and monitoring of malignant cancer using cancer care services and business analytics/cloud services. Using these services, the availability of patient data can be streamlined for further treatment. The use of smart devices and WSN can improve cancer care services by seamless and secure integration of the equipment used in chemotherapy procedures. Moreover, follow-up and monitoring can be shifted into the home through remote monitoring, process automation, and alert communication. In addition to this, WSNs can be employed in achieving better planning of treatment and finalizing appropriate prescription doses. All the systems including pharmacy, medical and radiation oncology servers may allow access to a detailed patient chart that can be enabled from any smart device *via* a remote VPN access from anywhere.

In another such study,<sup>124</sup> an ML-based classifier support vector machine (SVM) has been demonstrated for classifying the malignant and benign BrC by using a recursive feature selection algorithm to include more information from the dataset. The results reveal that the proposed algorithm identifies and selects the best subsets, and the SVM classifier reported optimal classification performance with 99% classification accuracy and specificity and 98% sensitivity. The proposed system is suitable for early detection of BrC with more effective recovery and treatment.



Salvi and Kadam<sup>125</sup> also presented an ML-based model, trained through CNN algorithm with 200 000 images. The study proposes that the raspberry pi-integrated thermal imaging sensor can be used by the patient to capture cancer cell images, which is further given as an input to the CNN trained model to identify the status of the image (benign or malignant). In addition, using the Wi-Fi and cloud technology, the captured images are wirelessly sent to the doctor for further examination.

Deep learning systems (DLSs) have been used to predict the presence of ER, PR, and HER2 using the 'patch level model' and hematoxylin-and-eosin-stained images as input.<sup>126</sup> The conventional and commercially existing methods employ costly preparation methods and produce inconstant scoring systems. Moreover, the contradiction in the histology and the expected biomarker results lead to repeated testing. In the study, computer software is trained to identify and classify the image features in order to find ER/PR/HER2 biomarkers in digitized images, instead of tissue stains. ML automatically predicts the status of the biomarkers in pathology images and further testing confirms the specific image features that assist in making the predictions. This method is cost-effective and less time consuming, and provides high-quality control in marker detection.

Despite the high advances made in various fields of cancer diagnostics, certain challenges need to be addressed. The most common of all issues is creating reproducible calibration and separation methods. Besides, identifying the appropriate technology while keeping the highest specificity and sensitivity is another challenge. Further, the device should offer the lowest detection time and detection limit with minimum consumption of energy and cost.<sup>127</sup> Research is also directed on identifying novel biomarkers using a single gene/protein for precise detection. It also includes the use of nanomaterial-based substrates along with a combination of different mechanisms on a common platform, resulting in multiple outputs from a single sensor.

Nanomaterials have a large surface-to-volume ratio that assists in better functionalization of the substrate for the binding of biomolecules, and thus, specific detection of cancer cells. Nanomaterial-based point-of-care devices have shown exceptionally low limit of detection towards the BrC biomarker HER-2.<sup>128–130</sup> Nanorobots are biocompatible, biodegradable, and biomimetic nanostructures that can detect and kill BrC cells. These can perform multiple tasks on a small scale, including targeted drug delivery and localized minimally invasive microsurgery. DNA nanorobots are specifically known to cause lysosomal degradation of BrC proteins, in different pH environments inside the cell and can also be used for imaging purposes through fluorescent tags.<sup>131</sup> Similarly, nanomotors,<sup>132</sup> nanobodies,<sup>132</sup> nanoflowers,<sup>133</sup> nanosubmarines,<sup>134</sup> nanotrains,<sup>135</sup> nanomachines, nanoballoons,<sup>136</sup> nanostars,<sup>137</sup> nanocages,<sup>138</sup> *etc.*, are all futuristic programmable DNA-based nanostructures that can be employed for safe imaging and

therapeutic purposes. These nanostructures can autonomously navigate throughout the body and are able to find and kill cancerous cells.<sup>139</sup> However, scalable fabrication or synthesis of nanomaterials is still a challenge. Moreover, the nanosafety concern must be developed to handle the unique and specific behavior of nanomaterials and further understand their potential toxicity.<sup>140</sup>

Most methods can identify one analyte at a time due to the limitation of a single biomarker. Therefore, for early diagnosis, simultaneous detection of multi-biomarkers is also necessary.<sup>141</sup> In the case of IoT-based solutions and systems, the issues of confidentiality and privacy are a major concern. Thus, it is imperative to ensure the operational and security challenges, about patient-sensitive information to avoid the breach of patient data. For this, it is necessary to ensure that all the connected devices conform to industry standards and provide necessary information with minimal equipment failure and lesser human intervention. AI, though a boom for medical diagnostics, requires a large amount and span of data sets to train the models. Thus, it will take some time for AI-based techniques to come up to full use till the current devices fetch, store and keep the data for the AI models.

## 6. Conclusion

Despite the conventional techniques still being used today for BrC diagnosis, there is a need for the development of pain-free, low-LOD, higher sensitivity and less-time-consuming methods. This review embraces various techniques (optical, mechanical, electrical, electrochemical, imaging, microwave, color based) and commercial techniques for BrC detection. The commercial options available to a future vision including AI and IoT techniques as a part of overcoming challenges for next-generation diagnostics of BrC are also included in the review. This review has furnished the working principle of techniques and works recently cited in the literature relevant to the above-mentioned methods. It renders all important information for scientists working in the field of BrC diagnostics.

## Data availability

No primary research results, software or code have been included, and no new data were generated or analysed as part of this review.

## Author contributions

Parikshana Mathur: writing – original draft, review and editing, visualization. Saakshi Dhanekar: conceptualization, supervision, writing – review and editing. B. D. Malhotra: writing – review and editing.

## Conflicts of interest

There are no conflicts to declare.



## Acknowledgements

The authors thank Shradha Suman Panda, Master's student in Medical Technologies Program in Smart Healthcare, IIT Jodhpur-AIIMS Jodhpur for helping in organizing a few topics for this manuscript.

## References

- L. Jing, C. Xie, Q. Li, M. Yang, S. Li and H. Li, *et al.*, Electrochemical Biosensors for the Analysis of Breast Cancer Biomarkers: From Design to Application, *Anal. Chem.*, 2022, **94**(1), 269–296, Available from: <https://pubs.acs.org/doi/10.1021/acs.analchem.1c04475>.
- Breast cancer [Internet], [cited 2024 Jul 15], Available from: <https://www.who.int/news-room/fact-sheets/detail/breast-cancer>.
- I. Abrao Nemeir, J. Saab, W. Hleihel, A. Errachid, N. Jafferzic-Renault and N. Zine, The Advent of Salivary Breast Cancer Biomarker Detection Using Affinity Sensors, *Sensors*, 2019, **19**(10), 2373.
- S. Afzal, M. Hassan, S. Ullah, H. Abbas, F. Tawakkal and M. A. Khan, Breast Cancer; Discovery of Novel Diagnostic Biomarkers, Drug Resistance, and Therapeutic Implications, *Front. Mol. Biosci.*, 2022, **9**, 783450.
- F. Aminolroayaei, S. Shahbazi-Gahrouei, A. Khorasani and D. Shahbazi-Gahrouei, A Review of Imaging Methods and Recent Nanoparticles for Breast Cancer Diagnosis, *Information*, 2023, **15**(1), 10.
- T. Mahmoudi, M. de la Guardia and B. Baradaran, Lateral flow assays towards point-of-care cancer detection: A review of current progress and future trends, *TrAC, Trends Anal. Chem.*, 2020, **125**, 115842.
- Z. Yang, X. Mao, M. Zhu, S. Chen, Z. Gao and T. Jiang, *et al.*, Chinese expert consensus on flow cytometric detection of hematological malignant cells in tissue samples, *J. Natl. Cancer Cent.*, 2025, **5**(1), 28–37.
- L. Vázquez-Iglesias, G. M. Stanfoca Casagrande, D. García-Lojo, L. Ferro Leal, T. A. Ngo and J. Pérez-Juste, *et al.*, SERS sensing for cancer biomarker: Approaches and directions, *Bioact. Mater.*, 2024, **34**, 248–268.
- M. Sharifi, A. Hasan, F. Attar, A. Taghizadeh and M. Falahati, Development of point-of-care nanobiosensors for breast cancers diagnosis, *Talanta*, 2020, **217**, 121091.
- A. Pulumati, A. Pulumati, B. S. Dwarakanath, A. Verma and R. V. L. Papineni, Technological advancements in cancer diagnostics: Improvements and limitations, *Cancer Rep.*, 2023, **6**(2), e1764, Available from: <https://onlinelibrary.wiley.com/doi/full/10.1002/cnr2.1764>.
- S. Mansouri, Y. Alharbi, F. Haddad, S. Chabcoub, A. Alshrouf and A. A. Abd-Elghany, Electrical Impedance Tomography – Recent Applications and Developments, *J. Electr. Bioimpedance*, 2021, **12**(1), 50, Available from: <https://pmc.ncbi.nlm.nih.gov/articles/PMC8667811/>.
- F. Achi, A. M. Attar and L. A. Ait, Electrochemical nanobiosensors for the detection of cancer biomarkers in real samples: Trends and challenges, *TrAC, Trends Anal. Chem.*, 2024, **170**, 117423.
- A. Krilaviciute, J. A. Heiss, M. Leja, J. Kupcinskas, H. Haick and H. Brenner, *et al.*, Detection of cancer through exhaled breath: a systematic review, *Oncotarget*, 2015, **6**(36), 38643–38657, Available from: <https://www.oncotarget.com/article/5938/text/>.
- P. Praveen and S. Lakshmi, *Cancer Detection Using MEMS Technology. 5th International Conference on Circuits, Control, Communication and Computing, IAC 2024*, 2024, 546–553.
- S. V. Joshi, S. Sadeghpour, N. Kuznetsova, C. Wang and M. Kraft, Flexible micromachined ultrasound transducers (MUTs) for biomedical applications, *Microsyst. Nanoeng.*, 2025, **11**(1), 1–21, Available from: <https://www.nature.com/articles/s41378-024-00783-5>.
- M. Aleixandre and M. C. Horrillo, Recent Advances in SAW Sensors for Detection of Cancer Biomarkers, *Biosensors*, 2025, **15**(2), 88, Available from: <https://www.mdpi.com/2079-6374/15/2/88/htm>.
- S. Akgönüllü, E. Özgür and A. Denizli, Quartz Crystal Microbalance-Based Aptasensors for Medical Diagnosis, *Micromachines*, 2022, **13**(9), 1441, Available from: <https://www.mdpi.com/2072-666X/13/9/1441/htm>.
- P. Jaglan, R. Dass and M. Duhan, Breast Cancer Detection Techniques: Issues and Challenges, *J. Inst. Eng. (India): B*, 2019, **100**(4), 379–386, Available from: <https://link.springer.com/article/10.1007/s40031-019-00391-2>.
- K. Lee, Optical mammography: Diffuse optical imaging of breast cancer, *World J. Clin. Oncol.*, 2011, **2**(1), 64–72, Available from: <http://www.ncbi.nlm.nih.gov/pubmed/21603315>.
- A. A. Abdul Halim, A. M. Andrew, M. N. Mohd Yasin, M. A. Abd Rahman, M. Jusoh and V. Veeraperumal, *et al.*, Existing and Emerging Breast Cancer Detection Technologies and Its Challenges: A Review, *Appl. Sci.*, 2021, **11**(22), 10753, Available from: <https://www.mdpi.com/2076-3417/11/22/10753/htm>.
- K. M. Koczula and A. Gallotta, Lateral flow assays, *Essays Biochem.*, 2016, **60**(1), 111–120.
- C. Liu, L. Yang, W. Zhang, D. Li, L. Li and H. Wang, *et al.*, A magnetic nanoparticle-based lateral flow immunochromatography assay for the rapid detection of fluoroquinolones in milk, *Eur. Food Res. Technol.*, 2021, **247**(10), 2645–2656, Available from: <https://link.springer.com/article/10.1007/s00217-021-03820-z>.
- V. Shirshahi, S. N. Tabatabaei, S. Hatamie and R. Saber, Functionalized reduced graphene oxide as a lateral flow immuneassay label for one-step detection of Escherichia coli O157:H7, *J. Pharm. Biomed. Anal.*, 2019, **164**, 104–111.
- L. Ye, X. Xu, A. Qu, L. Liu, C. Xu and H. Kuang, Quantitative assessment of the breast cancer marker HER2 using a gold nanoparticle-based lateral flow immunoassay, *Nano Res.*, 2024, **17**(6), 5452–5460, Available from: <https://link.springer.com/article/10.1007/s12274-024-6471-2>.



- 25 K. Deng, Z. L. Yu, X. Hu, J. Liu, X. Hong and G. G. L. Zi, *et al.*, NIR-II fluorescent Ag<sub>2</sub>Se polystyrene beads in a lateral flow immunoassay to detect biomarkers for breast cancer, *Microchim. Acta*, 2023, **190**(12), 1–9, Available from: <https://link.springer.com/article/10.1007/s00604-023-06039-9>.
- 26 Y. Wang, M. A. Ali, E. K. C. Chow, L. Dong and M. Lu, An optofluidic metasurface for lateral flow-through detection of breast cancer biomarker, *Biosens. Bioelectron.*, 2018, **107**, 224–229.
- 27 J. P. Robinson, R. Ostafe, S. N. Iyengar, B. Rajwa and R. Fischer, Flow Cytometry: The Next Revolution, *Cells*, 2023, **12**(14), 1875.
- 28 H. K. Mishra, Clinical Applications of Flow Cytometry in Cancer Immunotherapies: From Diagnosis to Treatments, in *Signal Transduction Immunohistochemistry*, ed. A. E. Kalyuzhny, Methods in Molecular Biology, Humana, New York, NY, 2023, vol. 2593, DOI: [10.1007/978-1-0716-2811-9\\_6](https://doi.org/10.1007/978-1-0716-2811-9_6).
- 29 K. Bhattacharyya, B. S. Goldschmidt and J. A. Viator, Detection and capture of breast cancer cells with photoacoustic flow cytometry, *J. Biomed. Opt.*, 2016, **21**(8), 087007, Available from: <https://pmc.ncbi.nlm.nih.gov/articles/PMC5005571/>.
- 30 W. Xu, Y. Zhang, D. Hou, J. Shen, J. Dong and Z. Gao, *et al.*, Quantitative SERS detection of multiple breast cancer miRNAs based on duplex specific nuclease-mediated signal amplification, *Anal. Methods*, 2023, **15**(24), 2915–2924, Available from: <https://pubs.rsc.org/en/content/articlehtml/2023/ay/d3ay00583f>.
- 31 L. Vázquez-Iglesias, G. M. Stanfoca Casagrande, D. García-Lojo, L. Ferro Leal, T. A. Ngo and J. Pérez-Juste, *et al.*, SERS sensing for cancer biomarker: Approaches and directions, *Bioact. Mater.*, 2024, **34**, 248–268.
- 32 V. Moisoiu, A. Stefancu, D. Gulei, R. Boitor, L. Magdo and L. Raduly, *et al.*, SERS-based differential diagnosis between multiple solid malignancies: breast, colorectal, lung, ovarian and oral cancer, *Int. J. Nanomed.*, 2019, **14**, 6165–6178.
- 33 V. Moisoiu, A. Socaciu, A. Stefancu, S. Iancu, I. Boros and C. Alecsa, *et al.*, Breast Cancer Diagnosis by Surface-Enhanced Raman Scattering (SERS) of Urine, *Appl. Sci.*, 2019, **9**(4), 806.
- 34 N. Gupta, S. Dhanekar, S. Chattopadhyay, S. S. Panda and H. Singh, An approach towards development of point of care diagnostics using ELISA, Proceedings of IEEE Sensors, 2021.
- 35 M. C. C. G. Carneiro, L. R. Rodrigues, F. T. C. Moreira and M. G. F. Sales, Paper-based ELISA for fast CA 15–3 detection in point-of-care, *Microchem. J.*, 2022, **181**, 107756.
- 36 J. W. Choi, B. I. Moon, J. W. Lee, H. J. Kim, Y. Jin and H. J. Kim, Use of CA15-3 for screening breast cancer: An antibody-lectin sandwich assay for detecting glycosylation of CA15-3 in sera, *Oncol. Rep.*, 2018, **40**(1), 145–154, Available from: <https://pubmed.ncbi.nlm.nih.gov/29749490/>.
- 37 J. Lee, B. Kim, B. Park, Y. Won, S. Y. Kim and S. Lee, Real-time cancer diagnosis of breast cancer using fluorescence lifetime endoscopy based on the pH, *Sci. Rep.*, 2021, **11**(1), 16864.
- 38 B. Kim, B. Park, S. Lee and Y. Won, GPU accelerated real-time confocal fluorescence lifetime imaging microscopy (FLIM) based on the analog mean-delay (AMD) method, *Biomed. Opt. Express*, 2016, **7**(12), 5055.
- 39 W. T. Dou, L. F. Liu, J. Gao, Y. Zang, G. R. Chen and R. A. Field, *et al.*, Fluorescence imaging of a potential diagnostic biomarker for breast cancer cells using a peptide-functionalized fluorogenic 2D material, *Chem. Commun.*, 2019, **55**(88), 13235–13238.
- 40 J. Eisermann, A. Kerth and D. Hinderberger, Dynamic self-assembly of ions with variable size and charge in solution, *RSC Adv.*, 2019, **9**(32), 18627–18640.
- 41 K. Glunde, Z. M. Bhujwala and S. M. Ronen, Choline metabolism in malignant transformation, *Nat. Rev. Cancer*, 2011, **11**(12), 835–848.
- 42 U. Sharma and N. R. Jagannathan, In vivo MR spectroscopy for breast cancer diagnosis, *BJR Open*, 2019, **1**(1), 20180040.
- 43 A. G. V. Bitencourt, J. Goldberg, K. Pinker and S. B. Thakur, Clinical applications of breast cancer metabolomics using high-resolution magic angle spinning proton magnetic resonance spectroscopy (HRMAS 1H MRS): systematic scoping review, *Metabolomics*, 2019, **15**(11), 148.
- 44 A. Bitencourt, V. Sevilimedu, E. A. Morris, K. Pinker and S. B. Thakur, Fat Composition Measured by Proton Spectroscopy: A Breast Cancer Tumor Marker?, *Diagnostics*, 2021, **11**(3), 564.
- 45 M. A. Bilal Ahmadani, S. Bhatti, Z. ul Abideen, M. S. Yaseen, T. Laique and J. Malik, Imaging in Breast Cancer: Use of Magnetic Resonance Spectroscopy, *Cureus*, 2020, **12**(8), e9734.
- 46 J. C. Gómez-Cortés, J. J. Díaz-Carmona, J. A. Padilla-Medina, A. E. Calderon, A. I. B. Gutiérrez and M. Gutiérrez-López, *et al.*, Electrical Impedance Tomography Technical Contributions for Detection and 3D Geometric Localization of Breast Tumors: A Systematic Review, *Micromachines*, 2022, **13**(4), 496.
- 47 Q. Dong, Y. Zhang, Q. He, C. Xu and X. Pan, Image reconstruction method for electrical impedance tomography based on RBF and attention mechanism, *Comput. Electr. Eng.*, 2023, **110**, 108826.
- 48 J. Lee, S. Gweon, K. Lee, S. Um, K. R. Lee and K. Kim, *et al.*, A 9.6 mW/Ch 10 MHz Wide-bandwidth Electrical Impedance Tomography IC with Accurate Phase Compensation for Breast Cancer Detection, in *2020 IEEE Custom Integrated Circuits Conference (CICC)*, IEEE, 2020, pp. 1–4.
- 49 S. Hong, K. Lee, U. Ha, H. Kim, Y. Lee and Y. Kim, *et al.*, A 4.9 mΩ-sensitivity mobile electrical impedance tomography IC for early breast-cancer detection system, *IEEE J. Solid-State Circuits*, 2015, **50**(1), 245–257.
- 50 H. H. Wan, H. Zhu, C. C. Chiang, J. S. Li, F. Ren and C. T. Tsai, *et al.*, High sensitivity saliva-based biosensor in detection of breast cancer biomarkers: HER2 and CA15-3, *J. Vac. Sci. Technol., B: Nanotechnol. Microelectron.: Mater., Process., Meas., Phenom.*, 2024, **42**(2), 023202.
- 51 C. O'Brien, C. K. Khor, S. Ardalan and A. Ignaszak, Multiplex electrochemical sensing platforms for the



- detection of breast cancer biomarkers, *Front. Med. Technol.*, 2024, **6**, 1360510.
- 52 A. A. Zare, H. Naderi-Manesh, S. M. Naghib, M. Shamsipur and F. Molaabasi, Label-free electrochemical cancer cell detection leveraging hemoglobin-encapsulated silver nanoclusters and Cu-MOF nanohybrids on a graphene-assisted dual-modal probe, *Sci. Rep.*, 2023, **13**(1), 21980.
  - 53 C. Pothipor, J. Jakmunee, S. Bamrungsap and K. Ounnunkad, An electrochemical biosensor for simultaneous detection of breast cancer clinically related microRNAs based on a gold nanoparticles/graphene quantum dots/graphene oxide film, *Analyst*, 2021, **146**(12), 4000–4009.
  - 54 P. Ranjan, M. Abubakar Sadique, S. Yadav and R. Khan, An Electrochemical Immunosensor Based on Gold-Graphene Oxide Nanocomposites with Ionic Liquid for Detecting the Breast Cancer CD44 Biomarker, *ACS Appl. Mater. Interfaces*, 2022, **14**(18), 20802–20812.
  - 55 H. Ilkhani, A. Ravalli and G. Marrazza, Design of an Affibody-Based Recognition Strategy for Human Epidermal Growth Factor Receptor 2 (HER2) Detection by Electrochemical Biosensors, *Chemosensors*, 2016, **4**(4), 23.
  - 56 M. Emami, M. Shamsipur, R. Saber and R. Irajirad, An electrochemical immunosensor for detection of a breast cancer biomarker based on antiHER2–iron oxide nanoparticle bioconjugates, *Analyst*, 2014, **139**(11), 2858–2866.
  - 57 Q. A. M. Al-Khafaji, M. Harris, S. Tombelli, S. Laschi, A. P. F. Turner and M. Mascini, *et al.*, An Electrochemical Immunoassay for HER2 Detection, *Electroanalysis*, 2012, **24**(4), 735–742.
  - 58 J. X. Zhang, C. L. Lv, C. Tang, A. J. Wang, L. P. Mei and P. Song, *et al.*, Sandwich-type ultrasensitive immunosensing of breast cancer biomarker based on core-shell Au@PdAg dog-bone-like nanostructures and Au@PtRh nanorods, *Sens. Actuators, B*, 2023, **382**, 133497.
  - 59 E. Arkan, R. Saber, Z. Karimi and M. Shamsipur, A novel antibody–antigen based impedimetric immunosensor for low level detection of HER2 in serum samples of breast cancer patients via modification of a gold nanoparticles decorated multiwall carbon nanotube-ionic liquid electrode, *Anal. Chim. Acta*, 2015, **874**, 66–74.
  - 60 A. Ravalli, C. G. da Rocha, H. Yamanaka and G. Marrazza, A label-free electrochemical affisensor for cancer marker detection: The case of HER2, *Bioelectrochemistry*, 2015, **106**, 268–275.
  - 61 L. Chun, S. E. Kim, M. Cho and W. Choe, *et al.*, Electrochemical detection of HER2 using single stranded DNA aptamer modified gold nanoparticles electrode, *Sens. Actuators, B*, 2013, **186**, 446–450.
  - 62 S. K. Arya, P. Zhurauski, P. Jolly, M. R. Batistuti, M. Mulato and P. Estrela, Capacitive aptasensor based on interdigitated electrode for breast cancer detection in undiluted human serum, *Biosens. Bioelectron.*, 2018, **102**, 106–112.
  - 63 R. C. B. Marques, S. Viswanathan, H. P. A. Nouws, C. Delerue-Matos and M. B. González-García, Electrochemical immunosensor for the analysis of the breast cancer biomarker HER2 ECD, *Talanta*, 2014, **129**, 594–599.
  - 64 S. Patris, P. De Pauw, M. Vandepuy, J. Huet, P. Van Antwerpen and S. Muyldermans, *et al.*, Nanoimmunoassay onto a screen printed electrode for HER2 breast cancer biomarker determination, *Talanta*, 2014, **130**, 164–170.
  - 65 C. Li, X. Qiu, D. Keqin and Z. Hou, Electrochemical co-reduction synthesis of Au/ferrocene–graphene nanocomposites and their application in an electrochemical immunosensor of a breast cancer biomarker. *Anal. Methods*, 2014, **6**(22), 9078–9084.
  - 66 H. Li, J. He, S. Li and A. P. F. Turner, Electrochemical immunosensor with N-doped graphene-modified electrode for label-free detection of the breast cancer biomarker CA 15-3, *Biosens. Bioelectron.*, 2013, **43**, 25–29.
  - 67 S. Ge, X. Jiao and D. Chen, Ultrasensitive electrochemical immunosensor for CA 15-3 using thionine-nanoporous gold–graphene as a platform and horseradish peroxidase-encapsulated liposomes as signal amplification, *Analyst*, 2012, **137**(19), 4440.
  - 68 W. Li, R. Yuan, Y. Chai and S. Chen, Reagentless amperometric cancer antigen 15-3 immunosensor based on enzyme-mediated direct electrochemistry, *Biosens. Bioelectron.*, 2010, **25**(11), 2548–2552.
  - 69 C. Hong, R. Yuan, Y. Chai and Y. Zhuo, Ferrocene-doped silica nanoparticles as an immobilized affinity support for electrochemical immunoassay of cancer antigen 15-3, *Anal. Chim. Acta*, 2009, **633**(2), 244–249.
  - 70 Y. Yang, Z. Zhong, H. Liu, T. Zhu, J. Wu and M. Li, *et al.*, Double-Layer Nanogold and Double-Strand DNA-Modified Electrode for Electrochemical Immunoassay of Cancer Antigen 15-3, *Electroanalysis*, 2008, **20**(24), 2621–2628.
  - 71 L. C. Ward and S. Brantlov, Bioimpedance basics and phase angle fundamentals, *Rev. Endocr. Metab. Disord.*, 2023, **24**(3), 381–391, Available from: <https://pubmed.ncbi.nlm.nih.gov/36749540/>.
  - 72 S. Mansouri, T. Alhadidi and M. B. Azouz, Breast Cancer Detection Using Low-Frequency Bioimpedance Device, *Breast Cancer: Targets Ther.*, 2020, **12**, 109–116, Available from: <https://www.dovepress.com/breast-cancer-detection-using-low-frequency-bioimpedance-device-peer-reviewed-fulltext-article-BCTT>.
  - 73 V. Cappelletti, E. Iorio, P. Miodini, M. Silvestri, M. Dugo and M. G. Daidone, Metabolic Footprints and Molecular Subtypes in Breast Cancer, *Dis. Markers*, 2017, **2017**, 1–19.
  - 74 P. Divyashree, H. A. Quadri, P. Dwivedi and S. Dhanekar, Demonstration of Intelligent Sensing by Nanosensors and use of Classification and Regression Models for Electronic Nose Applications, *IEEE Sens. J.*, 2024, **24**(21), 35423–35428.
  - 75 H. Y. Yang, Y. C. Wang, H. Y. Peng and C. H. Huang, Breath biopsy of breast cancer using sensor array signals and machine learning analysis, *Sci. Rep.*, 2021, **11**(1), 1–9, Available from: <https://www.nature.com/articles/s41598-020-80570-0>.



- 76 J. Liu, H. Chen, Y. Li, Y. Fang, Y. Guo and S. Li, *et al.*, A novel non-invasive exhaled breath biopsy for the diagnosis and screening of breast cancer, *J. Hematol. Oncol.*, 2023, **16**(1), 1–5, Available from: <https://jhoonline.biomedcentral.com/articles/10.1186/s13045-023-01459-9>.
- 77 O. Barash, W. Zhang, J. M. Halpern, Q. L. Hua, Y. Y. Pan and H. Kayal, *et al.*, Differentiation between genetic mutations of breast cancer by breath volatolomics, *Oncotargets Ther.*, 2015, **6**(42), 44864–44876.
- 78 L. Lavra, A. Catini, A. Ulivieri, R. Capuano, L. Baghernajad Salehi and S. Sciacchitano, *et al.*, Investigation of VOCs associated with different characteristics of breast cancer cells, *Sci. Rep.*, 2015, **5**(1), 13246.
- 79 C. B. Ambrosone, Oxidants and Antioxidants in Breast Cancer, *Antioxid. Redox Signaling*, 2000, **2**(4), 903–917.
- 80 O. Herman-Saffar, Z. Boger, S. Libson, D. Lieberman, R. Gonen and Y. Zeiri, Early non-invasive detection of breast cancer using exhaled breath and urine analysis, *Comput. Biol. Med.*, 2018, **96**, 227–232.
- 81 L. D. De León-Martínez, M. Rodríguez-Aguilar, P. Gorocica-Rosete, C. A. Domínguez-Reyes, V. Martínez-Bustos and J. A. Tenorio-Torres, *et al.*, Identification of profiles of volatile organic compounds in exhaled breath by means of an electronic nose as a proposal for a screening method for breast cancer: a case-control study, *J. Breath Res.*, 2020, **14**(4), 046009, Available from: <https://iopscience.iop.org/article/10.1088/1752-7163/aba83f>.
- 82 M. J. Madou, *Fundamentals of Microfabrication and Nanotechnology, Three-Volume Set*, 2018, Available from: <https://www.taylorfrancis.com/books/mono/10.1201/9781315274164/fundamentals-microfabrication-nanotechnology-three-volume-set-marc-madou>.
- 83 A. V. G. K., G. Gogoi, B. Behera, S. Rila, A. Rangarajan and H. J. Pandya, RapidET: a MEMS-based platform for label-free and rapid demarcation of tumors from normal breast biopsy tissues, *Microsyst. Nanoeng.*, 2022, **8**(1), 1.
- 84 I. Acerbi, L. Cassereau, I. Dean, Q. Shi, A. Au and C. Park, *et al.*, Human breast cancer invasion and aggression correlates with ECM stiffening and immune cell infiltration, *Integr. Biol.*, 2015, **7**(10), 1120–1134.
- 85 E. Leikina, M. V. Merts, N. Kuznetsova and S. Leikin, Type I collagen is thermally unstable at body temperature, *Proc. Natl. Acad. Sci. U. S. A.*, 2002, **99**(3), 1314–1318.
- 86 N. Ignatieva, O. Zakharkina, A. Dadasheva, A. Shekhter, A. Sviridov and V. Lunin, Transformation of the dermal collagen framework under laser heating, *J. Biophotonics*, 2019, **12**(12), e201960024.
- 87 A. Khosla, MEMS Based Eit Technology for Non-Invasive Breast Cancer Diagnostics, *ECS Meeting Abstracts*, 2014, **02**(11), 690, Available from: <https://iopscience.iop.org/article/10.1149/MA2014-02/11/690>.
- 88 A. V. Anil, G. Gogoi, B. Behera, S. Rila, A. Rangarajan and H. J. Pandya, RapidET: a MEMS-based platform for label-free and rapid demarcation of tumors from normal breast biopsy tissues, *Microsyst. Nanoeng.*, 2022, **8**(1), 1–16, Available from: <https://www.nature.com/articles/s41378-021-00337-z>.
- 89 L. Arcarisi, L. Di Pietro, N. Carbonaro, A. Tognetti, A. Ahluwalia and C. De Maria, Palpreast—A New Wearable Device for Breast Self-Examination, *Appl. Sci.*, 2019, **9**(3), 381.
- 90 J. Jung, W. Lee, W. Kang, E. Shin, J. Ryu and H. Choi, Review of piezoelectric micromachined ultrasonic transducers and their applications, *J. Micromech. Microeng.*, 2017, **27**(11), 113001.
- 91 L. Li, J. Zheng, J. Chen, Z. Luo, Y. Su and W. Tang, *et al.*, Flexible Pressure Sensors for Biomedical Applications: From Ex Vivo to In Vivo, *Adv. Mater. Interfaces*, 2020, **7**(17), 2000743, Available from: <https://onlinelibrary.wiley.com/doi/full/10.1002/admi.202000743>.
- 92 C. Liu, C. Xue, B. Zhang, G. Zhang and C. He, The Application of an Ultrasound Tomography Algorithm in a Novel Ring 3D Ultrasound Imaging System, *Sensors*, 2018, **18**(5), 1332.
- 93 K. Chang, Y. Pi, W. Lu, F. Wang, F. Pan and F. Li, *et al.*, Label-free and high-sensitive detection of human breast cancer cells by aptamer-based leaky surface acoustic wave biosensor array, *Biosens. Bioelectron.*, 2014, **60**, 318–324.
- 94 W. Geng, Y. Liu, N. Yu, X. Qiao, M. Ji and Y. Niu, *et al.*, An ultra-compact acoustofluidic device based on the narrow-path travelling surface acoustic wave (np-TSAW) for label-free isolation of living circulating tumor cells, *Anal. Chim. Acta*, 2023, **1255**, 341138.
- 95 A. Karczmarczyk, K. Haupt and K. H. Feller, Development of a QCM-D biosensor for Ochratoxin A detection in red wine, *Talanta*, 2017, **166**, 193–197.
- 96 M. Bakhshpour, A. K. Piskin, H. Yavuz and A. Denizli, Quartz crystal microbalance biosensor for label-free MDA MB 231 cancer cell detection via notch-4 receptor, *Talanta*, 2019, **204**, 840–845.
- 97 M. Yılmaz, M. Bakhshpour, I. Göktürk, A. K. Pişkin and A. Denizli, Quartz Crystal Microbalance (QCM) Based Biosensor Functionalized by HER2/neu Antibody for Breast Cancer Cell Detection, *Chemosensors*, 2021, **9**(4), 80.
- 98 N. Köü, A. Köü, M. Duran, S. Simavlı and N. Turhan, Comparison of standard mammography with digital mammography and digital infrared thermal imaging for breast cancer screening Meme kanseri taramasında standart mamografi ile dijital mamografi ve dijital infrared termal görüntülemenin karlatılması, *J. Turk.-Ger. Gynecol. Assoc.*, 2010, **11**, 152–159.
- 99 Y. R. Parisky, A. Sardi, R. Hamm, K. Hughes, L. Esserman and S. Rust, *et al.*, Efficacy of Computerized Infrared Imaging Analysis to Evaluate Mammographically Suspicious Lesions, *AJR, Am. J. Roentgenol.*, 2003, **180**(1), 263–269.
- 100 S. Ekici and H. Jawzal, Breast cancer diagnosis using thermography and convolutional neural networks, *Med. Hypotheses*, 2020, **137**, 109542.
- 101 R. Resmini, L. Silva, A. S. Araujo, P. Medeiros, D. Muchaluat-Saade and A. Conci, Combining Genetic Algorithms and SVM for Breast Cancer Diagnosis Using Infrared Thermography, *Sensors*, 2021, **21**(14), 4802.



- 102 S. Tello-Mijares, F. Woo and F. Flores, Breast Cancer Identification via Thermography Image Segmentation with a Gradient Vector Flow and a Convolutional Neural Network, *J. Healthc. Eng.*, 2019, **2019**, 1–13.
- 103 L. V. Wang and H. I. Wu, Definitions of Optical Properties, *Biomedical Optics: Principles and Imaging*, 2007, pp. 343–346, Available from: <https://www.wiley.com/en-us/Biomedical+Optics%3A+Principles+and+Imaging-p-9780471743040>.
- 104 E. Y. Chae, H. H. Kim, S. Sabir, Y. Kim, H. Kim and S. Yoon, *et al.*, Development of digital breast tomosynthesis and diffuse optical tomography fusion imaging for breast cancer detection, *Sci. Rep.*, 2020, **10**(1), 13127.
- 105 J. E. McGuinness, M. L. Altoe, A. Marone, L. E. Franks, S. M. Lee and H. K. Kim, *et al.*, Diffuse optical tomography breast imaging measurements are modifiable with pre-surgical targeted and endocrine therapies among women with early stage breast cancer, *Breast Cancer Res. Treat.*, 2021, **189**(1), 297–304, Available from: <https://link.springer.com/article/10.1007/s10549-021-06320-6>.
- 106 Y. Wang, Y. Wang, S. Li, S. Li, Y. Wang and Q. Yan, *et al.*, Compact fiber-free parallel-plane multi-wavelength diffuse optical tomography system for breast imaging, *Opt. Express*, 2022, **30**(5), 6469–6486, Available from: <https://opg.optica.org/viewmedia.cfm?uri=oe-30-5-6469&seq=0&html=true>.
- 107 D. N. Elsheakh, R. A. Mohamed, O. M. Fahmy, K. Ezzat and A. R. Eldamak, Complete Breast Cancer Detection and Monitoring System by Using Microwave Textile Based Antenna Sensors, *Biosensors*, 2023, **13**(1), 87.
- 108 E. C. Fear, P. M. Meaney and M. A. Stuchly, *Microwaves for breast cancer detection? IEEE Potentials*, 2003, 221, pp. 12–18.
- 109 L. Wang, Microwave Imaging and Sensing Techniques for Breast Cancer Detection, *Micromachines*, 2023, **14**(7), 1462, Available from: <https://www.mdpi.com/2072-666X/14/7/1462/htm>.
- 110 M. T. Islam, M. Z. Mahmud, M. T. Islam, S. Kibria and M. Samsuzzaman, A Low Cost and Portable Microwave Imaging System for Breast Tumor Detection Using UWB Directional Antenna array, *Sci. Rep.*, 2019, **9**(1), 15491.
- 111 IEEE Xplore, Full-Text PDF: [Internet], [cited 2024 May 16], Available from: <https://ieeexplore.ieee.org/stamp/stamp.jsp?tp=&number=7384493>.
- 112 Hello - The Blue Box Biomedical Solutions, S.L. [Internet], [cited 2024 May 17], Available from: <https://thebluebox.ai/>.
- 113 BRCA1 elisa kit | Human Breast Cancer Susceptibility Protein 1 ELISA Kit-AAC37594.1.
- 114 ab108633 Cancer Antigen CA15-3 Human ELISA Kit Instructions for Use.
- 115 HercepTest Kits | Agilent [Internet], [cited 2024 May 17], Available from: <https://www.agilent.com/en/product/pharmdx/herceptest-kits>.
- 116 Xpert® Breast Cancer STRAT4 [Internet], [cited 2024 May 17], Available from: <https://www.cepheid.com/en-GB/tests/oncology-human-genetics/xpert-breast-cancer-strat4.html>.
- 117 G. Jian, S. Zhu, X. Yuan, S. Fu, N. Yang and C. Yan, *et al.*, Biodegradable triboelectric nanogenerator as a implantable power source for embedded medicine devices, *NPG Asia Mater.*, 2024, **16**(1), 12.
- 118 S. Solanki, A. K. Gupta, U. Saha, A. V. Krasnoslobodtsev, R. K. Gupta and B. D. Malhotra, Triboelectric Nanogenerator-based smart biomedical sensors for healthcare, *Sustain. Energy Technol. Assessments*, 2023, **57**, 103233.
- 119 B. Gil, S. Anastasova and G. Z. Yang, Low-powered implantable devices activated by ultrasonic energy transfer for physiological monitoring in soft tissue via functionalized electrochemical electrodes, *Biosens. Bioelectron.*, 2021, **182**, 113175.
- 120 S. S. Rao, G. G. Bushnell, S. M. Azarin, G. Spicer, B. A. Aguado and J. R. Stoehr, *et al.*, Enhanced Survival with Implantable Scaffolds That Capture Metastatic Breast Cancer Cells In Vivo, *Cancer Res.*, 2016, **76**(18), 5209–5218.
- 121 A. R. K. Sasikala, A. R. Unnithan, R. G. Thomas, S. W. Ko, Y. Y. Jeong and C. H. Park, *et al.*, Multifaceted Implantable Anticancer Device for Potential Postsurgical Breast Cancer Treatment: A Single Platform for Synergistic Inhibition of Local Regional Breast Cancer Recurrence, Surveillance, and Healthy Breast Reconstruction, *Adv. Funct. Mater.*, 2018, **28**(8), 1704793.
- 122 R. Jalloul, H. K. Chethan and R. Alkhatib, A Review of Machine Learning Techniques for the Classification and Detection of Breast Cancer from Medical Images, *Diagnostics*, 2023, **13**(14), 2460.
- 123 A. Onasanya and M. Elshakankiri, Smart integrated IoT healthcare system for cancer care, *Wireless Networks*, 2021, **27**(6), 4297–4312.
- 124 M. H. Memon, J. P. Li, A. U. Haq, M. H. Memon and W. Zhou, Breast Cancer Detection in the IOT Health Environment Using Modified Recursive Feature Selection, *Wirel. Commun. Mob. Comput.*, 2019, **2019**, 1–19.
- 125 S. Salvi and A. Kadam, Breast Cancer Detection Using Deep learning and IoT Technologies, *J. Phys.: Conf. Ser.*, 2021, **1831**, 012030.
- 126 P. Gamble, R. Jaroensri, H. Wang, F. Tan, M. Moran and T. Brown, *et al.*, Determining breast cancer biomarker status and associated morphological features using deep learning, *Commun. Med.*, 2021, **1**(1), 14.
- 127 M. Sadeghi, S. Sadeghi, S. M. Naghib and H. R. Garshasbi, A Comprehensive Review on Electrochemical Nano Biosensors for Precise Detection of Blood-Based Oncomarkers in Breast Cancer, *Biosensors*, 2023, **13**(4), 481.
- 128 S. Augustine, P. Kumar and B. D. Malhotra, Amine-Functionalized MoO<sub>3</sub>@RGO Nanohybrid-Based Biosensor for Breast Cancer Detection, *ACS Appl. Bio Mater.*, 2019, **2**(12), 5366–5378.
- 129 S. Augustine, A. G. Joshi, B. K. Yadav, A. Mehta, P. Kumar and V. Renugopalakrishnan, *et al.*, An emerging nanostructured molybdenum trioxide-based biocompatible



- sensor platform for breast cancer biomarker detection, *MRS Commun.*, 2018, **8**(3), 668–679, Available from: <https://link.springer.com/article/10.1557/mrc.2018.182>.
- 130 M. A. Ali, K. Mondal, C. Singh, B. Dhar Malhotra and A. Sharma, Anti-epidermal growth factor receptor conjugated mesoporous zinc oxide nanofibers for breast cancer diagnostics, *Nanoscale*, 2015, **7**(16), 7234–7245, Available from: <https://pubs.rsc.org/en/content/articlehtml/2015/nr/c5nr00194c>.
- 131 R. Arvidsson and S. F. Hansen, Environmental and health risks of nanorobots: an early review, *Environ. Sci.: Nano*, 2020, **7**(10), 2875–2886.
- 132 H. Bakherad, F. Ghasemi, M. Hosseindokht and H. Zare, Nanobodies; new molecular instruments with special specifications for targeting, diagnosis and treatment of triple-negative breast cancer, *Cancer Cell Int.*, 2022, **22**(1), 245.
- 133 H. Patel, K. Parekh, L. Fernel Gamarra, J. Bustamante Mamani, A. A. da Hora and A. M. Figueiredo Neto, In vitro evaluation of magnetic fluid hyperthermia therapy on breast cancer cells using monodispersed Mn<sub>0.5</sub>Zn<sub>0.5</sub>Fe<sub>2</sub>O<sub>4</sub> nanoflowers, *J. Magn. Magn. Mater.*, 2023, **587**, 171275.
- 134 M. Pumera, Electrochemically powered self-propelled electrophoretic nanosubmarines, *Nanoscale*, 2010, **2**(9), 1643.
- 135 Z. Xu, R. Ni and Y. Chen, Targeting breast cancer stem cells by a self-assembled, aptamer-conjugated DNA nanotrain with preloading doxorubicin, *Int. J. Nanomed.*, 2019, **14**, 6831–6842.
- 136 B. Xie, X. Yang, R. Zhang, J. Guo, Z. Chen and Y. He, Hollow and Porous Fe<sub>3</sub>C-NC Nanoballoons Nanozymes for Cancer Cell H<sub>2</sub>O<sub>2</sub> Detection, *Sens. Actuators, B*, 2021, **347**, 130597.
- 137 M. K. Hameed, J. B. M. Parambath, M. T. Gul, A. A. Khan, Y. Park and C. Han, *et al.*, Arylated gold nanostars aided SERS study of breast cancer cells, *Appl. Surf. Sci.*, 2022, **583**, 152504.
- 138 P. Ji, X. Wang, J. Yin, Y. Mou, H. Huang and Z. Ren, Selective delivery of curcumin to breast cancer cells by self-targeting apoferritin nanocages with pH-responsive and low toxicity, *Drug Delivery*, 2022, **29**(1), 986–996.
- 139 A. N. Neagu, T. Jayaweera, K. Weraduwage and C. C. Darie, A Nanorobotics-Based Approach of Breast Cancer in the Nanotechnology Era, *Int. J. Mol. Sci.*, 2024, **25**(9), 4981.
- 140 F. Lebre, N. Chatterjee, S. Costa, E. Fernández-de-Gortari, C. Lopes and J. Meneses, *et al.*, Nanosafety: An Evolving Concept to Bring the Safest Possible Nanomaterials to Society and Environment, *Nanomaterials*, 2022, **12**(11), 1810.
- 141 B. Kaur, S. Kumar and B. K. Kaushik, Recent advancements in optical biosensors for cancer detection, *Biosens. Bioelectron.*, 2022, **197**, 113805.

